RSC Advances

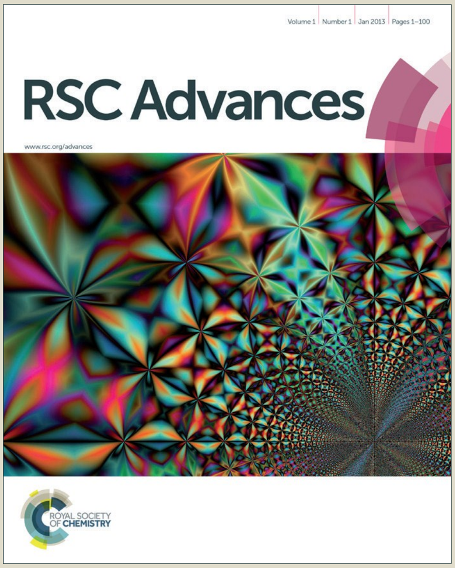

ROYAL SOCIETY OF CHEMISTRY

www.rsc.org/advances

Research Progress on Methane Production from Natural Gas Hydrates

Chun-Gang Xu and Xiao-Sen Li[1][a]

[a]*Key Laboratory of Gas Hydrate, Guangzhou Institute of Energy Conversion, Chinese Academy of Sciences, Guangzhou 510640, People's Republic of China*

Abstract: With the consumption of fossil fuels, an alternative energy becomes necessary for world's continuous development. Methane hydrates as a vast energy resource, which exists in deep-ocean or permafrost sediments contains approximately 10,000 Gt of carbon, is a potential energy in the future. However, economically and safely producing methane from gas hydrate deposits is still not on the drawing board. The main reasons include (1) low methane production efficiency, (2) low methane production, (3) poor production sustainability. Thus, it is pressing to develop methane production technology and/or approaches and to improve the methane production efficiency. In this paper, we comprehensively review the research on methane production from the gas hydrates, including the researches of characteristics of gas hydrate reservoirs, production methods, numerical simulation and field production tests. The different researches are interviewed and analyzed, and the relevant comments and suggestion are proposed accordingly.

Keywords: Gas Hydrate, Methane Production, Numerical Simulation, Fossil Fuels, Energy

Introduction

As the consumption of fossil fuels, an alternative energy becomes necessary for world's continuous development. Natural gas hydrate (NGH) is regarded as a potential future resource for its wide existence in ocean floor and permafrost zones, containing approximately carbon of 10,000 Gt[1-5]. Presently, the explored NGH reservoirs in the oceanic floor mainly distribute

---

[a]*Key Laboratory of gas hydrate, Guangzhou Institute of Energy Conversion, Chinese Academy of Sciences, Guangzhou 510640, People's Republic of China*
Tel: (+86)20-87057037; Fax: (+86)20-87034664
E-mail:lixs@ms.giec.ac.cn

in Japan, India, Gulf of Mexico, Bering Strait, South China Sea, Korea, Trinida And Tobago, and those in the permafrost mainly distribute in Alaska (USA), Mackenzie Delta (CAN), Qinghai-Tibet plateau (China) and Siberia (RUS)[6]. NGH is an non-stoichiometric crystalline compound, which consists of natural gas molecules and water molecules in the condition of high pressure and low temperature[7]. The characteristics of the NGH change with the condition of NGH reservoir. The basis of production of natural gas from the NGH is shifting the equilibrium condition of the NGH reservoir to the NGH dissociation side[8, 9], Therefore, a number of the scientific issues concerning NGH decomposition were discussed[10-14].

The NGH as a potential energy for future is in solid form and not amenable to the conventional gas and oil production techniques[15]. Thus, before the experimental production simulation, researchers still need to do a large amount of numerical simulation work to predetermine or evaluate the feasibility of the gas production from the NGH. The key parameters for preparing the numerical simulation include the properties of the reservoir, boundary conditions, structure of NGH. The NGH deposits are mainly divided into three classes[16-18]. Class 1 is composed of the Hydrate-Bearing Layer (HBL) and an underlying two-phase fluid zone with free gas. Class 2 consists of an HBL and an underlying zone of mobile water. Class 3 only contains an HBL, no underlying zone of mobile fluids. Additionally, there is a forth classification, Class 4. The Class 4 only disperses in oceanic floor with low hydrate saturation and lacks confining geologic strata[19]. The different NGH deposits mean different reservoirs with various properties, resulting in different boundary conditions for either numerical simulation or experimental production. Presently, the most popular production approaches involve depressurization, heating (thermal stimulation), chemical inhibition injection, and their combinations[20].

The depressurization is lowering the inside pressure of the well and promoting the NGH to dissociate, and further lowering the pressure in the free-gas zone rapidly beneath that in the hydrate stability zone, decomposing the hydrates in the stability zone. The study of experimental simulation production is conducted in a confined reservoir, and a depressurizing downhole well is drilled in the reservoir. During the depressurization, the decomposed natural gases flow from the hydrate deposits to the well[21]. However, the NGH dissociation is an endothermic process, which results in the decrease of the temperature and even prevents the

NGH from continuously dissociating. Thus, it is important to maintain the temperature by heat supply from outside or heat exchange during the depressurization. Additionally, the gas production from NGH is accompanied by the large production of water, and the spread or the flow of the water must impact on the properties of the system and the natural gas recovery.

The thermal stimulation is injecting heat source (e.g., hot water, steam) into the hydrate stability zone to raise its temperature and decompose NGH. The decomposed natural gases mixed with the hot water or the steam return the surface. For the thermal stimulation, the diffusion of the heat sources in the hydrate zone and the heat exchange efficiency are important[22].However, compared to the depressurization, the thermal stimulation is quite expensive because of the consumption of large amount of heat energy. Researchers are seeking to a new and economical integrated method which combines the depressurization with the thermal simulation[23-25].

The method of chemical inhibition injection seeks to shift the NGH equilibrium condition by injecting chemical inhibition into the NGH reservoir. The popular chemical inhibitions include alcohol (e.g., methanol, glycol) and electrolyte (e.g., Calcium Chloride - $CaCl_2$)[26-30]. The inhibition is injected directly from surface down to the NGH layers. However, because the chemical inhibition contaminates the environment and the production rate by the method is slow, the method does not attract more attention instead of CO_2 injection. Presently, the projects of injecting CO_2 into the NGH deposits to replace methane from the NGH are extensively being studied [31-34]. After the thermodynamic feasibility of the replacement between CO_2 and methane (CH_4) in hydrates has been proved[35-39], the various studies on the replacement of methane hydrate with CO_2 have been or are being conducted, including molecular dynamics simulation[40-43], kinetic model[36, 44], and experimental replacement[45-51]. Relative to the other methods, the method of replacement of methane from NGHs with CO_2 does not only seek to produce methane from the NGHs but also sequestrate CO_2 directly. However, the low replacement rate and low CH_4 recovery illustrate that the studies are still in its infancy, and too much work need to be done in the future.

Of all these production technologies, the depressurization is considered as the simplest one, and it is especially suitable for the zones where free-gas is trapped beneath the methane hydrates. The method of depressurization combined with heating seems to be the most practical. Currently, many countries including USA, Canada, Japan, Russia, China, India, etc., have proposed projects on drilling and producing NGHs. In 2002, the First Onshore Production Test was carried out in Mallik site in the Mackenzie Delta in the Northwest Territories of Canada. In the test, the “hot water circulation method” - a method of heating – was adopted for producing methane gas from NGH. This was the first time in the world that anyone had ever produced methane gas from methane hydrate layers. Five years later, the depressurization method was used for the tests of producing methane from NGH in the same site in 2007 and 2008. The tests demonstrated the depressurization is more effective for producing NGH relative to the heat stimulation [52]. In 2013, Japan said it has successfully extracted natural gas from frozen methane hydrate off its central coast (Nankai trough) by the depressurization, and it was the first offshore production [53].

However, there is no any large-scale industrial production in the world. In fact, the methane production from NGH is still a long-term research work. In this paper, the reported studies are reviewed systematically and comprehensively from the aspects of properties of hydrate deposits, numerical simulation production, experimental simulation production and molecular dynamics simulation, etc. And we hope to highlight the focus of the next research through this paper.

Classification of NGH Reservoirs

NGH is formed if natural gas and water coexist in the low temperature and high pressure conditions satisfying NGH stability. According to the differences of the places and the forms of gas and water existing, NGH deposits are defined as three types (as shown in Figure 1), pore filling type NGH reservoir, naturally fractured type NGH reservoir and massive/nodule NGH reservoir[16]. Figure 2 shows the real NGH deposits with different morphologies which were drilled out in different areas[54]. In the first type, NGH, like a typical accumulation of conventional oil and gas, is contained in pore spaces of porous media such as sandstones and carbonate rocks. In the second type, NGH is contained in fractures or veins. And in the third type, NGH is accumulated in the form of lump in fine grained muds, probably because of the formation of NGH on the surface of sea floor. Among all the presently proven NGH reservoirs, the Mallik NGH reservoirs in Canada where the onshore production tests were carried out with the success of the world first sustainable gas production from NGH reservoirs, Mt. Elbert NGH reservoirs in Alaska North Slope where the reservoir characteristics were investigated by analyzing the data acquired through exploratory drilling, coring and well logging, and reservoirs located in the Eastern Nankai Trough offshore Japan where NGH was confirmed by 2D/3D seismic and exploratory drilling camps were categorized into the first type, the pore filling NGH reservoir [55-57]. The second fracture type NGH reservoirs were discovered in offshore India and offshore Korea, and the third massive/nodule NGH reservoirs were confirmed in Gulf of Mexico and in Japan Sea. However, it is quite difficult to produce gas from both the second and the third types of NGH reservoirs, probably due to the relatively low energy efficiency. And as illustrated in Figure 3, the two types reservoirs are ranked as a few levels below the pore filling type NGH reservoirs as energy resources[58].Figure 3 shows a resource pyramid proposed by Boswell and Collett in 2006[58]. The resource pyramid displays the relative size and feasibility for production of the different categories of NGH occurrences in nature. Thus, the following contents focus on discussions of the pore filling type NGH.

In terms of the conditions of the existence of NGH, free gas and free water, the pore filling type reservoirs are further divided into four main classes. Class 1 accumulations comprise two zones: the hydrate interval, which generally exhibits a very low effective permeability because of the presence of large hydrate saturations in the pore space, and an underlying two-phase fluid zone with free gas. In this class, the bottom of the hydrate stability zone usually is consistent with the bottom of the hydrate interval. In the aspect of methane production, Class 1 is the most desirable class for exploitation owing to the hydrate thermodynamic proximity to the hydrate equilibrium, in other words, only small changes in pressure and temperature are necessitated to induce NGH dissociation. Messoyakha Field in Russia and Sagavanirktok Formation in Alaska are typical examples of Class 1 deposits. Class 2 deposits feature two zones, including a hydrate-bearing interval and a mobile water zone with no free gas (e.g. an aquifer) overlying the hydrate-bearing interval. Class 3 deposits include only a single zone, the hydrate interval, and they are typically characterized by the absence of an underlying zone of mobile fluids. Most of NGH deposits discovered in the Eastern Nankai Trough, Mallik site and Mt. Elbert are categorized into Class 3 NGH deposits, and a part of reservoirs in the Eastern Nankai Trough and the Mallik site are Class 2 NGH deposits. Different from the above three Class deposits, Class 4 deposits are widespread and not bounded by confining strata, and they mainly appear as nodules with low saturation over large areas. Moridis et al.[9] defined Class 4 deposits as those NGH deposits containing NGH sparsely in mud layers. Currently, the Class 4 deposits are generally not regarded as a target for exploitation. The schematic over Class 1~3 types of the NGH deposits is shown in Figure 4. In Classes 2 and 3, the entire hydrate interval might be well within the hydrate stability zone, that is to say, the bottom of the hydrate interval does not mark the bottom of the hydrate stability zone. Relative to the NGH deposit of Class 1, the desirability of Classes 2 and 3 accumulations as gas production targets is not well defined, and it could be affected by many factors such as thermodynamic proximity to hydration equilibrium, initial conditions of temperature, pressure and boundary, environ-mental concerns and economic considerations[59].

In the four NGH deposits, the NGH dissociation and gas production are highly related to the properties of the porous media such as sand layers, sandstones and carbonate rocks[60, 61]. The parameters, including depth, thickness, porosity, permeability, NGH saturation, thermodynamic conductivity, initial conditions of temperature, pressure and boundary, are essential to evaluating the gas producibility from the NGH reservoirs. Besides the parameters, heterogeneities of the NGH reservoir such as spatial variation of permeability and NGH saturation, and distribution of impermeable layers are quite important to the gas production from the NGH reservoir. In the pore filling type NGH reservoir, for example, the properties of the type reservoirs range widely: the reservoirs with depth from 1000 m to 1500 m, thickness from a few meters to over 100 m, porosity from a few percent to over 40%, absolute permeability from a few milidarcy to over 1000 mD, initially effective permeability to water in the presence of NGH from almost zero to over 10 mD, NGH saturation from almost zero to over 90%, the total thermal conductivity from 2 W/mK to 4 W/mK, the initial temperature and pressure from 3℃ to 15℃ and 5 MPa to 15 MPa, respectively[60].

Gas Production Methods

For a certain NGH reservoir, the initial temperature and pressure are in the NGH stability conditions. To dissociate NGH and produce gas from the NGH reservoir, it is necessary to shift the initial temperature and pressure to the NGH dissociation side. As depicted in Figure 5, the depressurization decreases a NGH reservoir pressure below three-phase (Gas-NGH-Water) equilibrium pressure, while thermal injection increases temperature above three-phase equilibrium temperature. Inhibitor injection shifts the three-phase equilibrium conditions to the high pressure and low temperature, thereby, moves reservoir conditions to the NGH dissociation side. Presently, new methods combined the above three basic methods are proposed to enhance gas production from a NGH reservoir. Besides, several other methods such as CO_2 injection, electrical heating and irradiation of ultrasonic wave are also investigated especially for the NGH dissociation and gas production[62-64]. Figure 6 shows the schematic of the three main gas production methods, and in the figure, pictures (a), (b) and (c) are depressurization, hot injection and inhibitor injection, respectively. The features of these methods are briefly described in the following.

Depressurization method

For depressurization, the pressure in bottomhole is reduced by a pump installed in the downhole. As the bottomhole pressure is lower than the three-phase equilibrium pressure, the NGH in the reservoir dissociates to release natural gas, then, the NGH dissociation starts from the regions near well. Along with the dissociation of NGH and hence with the decrease in NGH saturation, effective permeability to fluids increases remarkably, which results in the low pressure being more easily transferred to the regions more distant from the well. Thereby, a virtuous cycle is formed as (low pressure transfer→ NGH dissociation → increase in permeability → low pressure transfer to more distant area from well → more NGH dissociation → more increase in permeability→ and so on) in the depressurization method, and by the cycle, the areas of NGH dissociation and gas production hence increase with time. However, because the dissociation of NGH is an endothermic reaction, the reservoir temperature must decrease along with the NGH dissociation. Thus, once the reservoir temperature is lower than or even identical to the three-phase equilibrium temperature corresponding to the reservoir pressure, the NGH dissociation stops, and the gas production hence stops. Therefore, with the depressurization method, the sustainability of gas production depends on the temperature transfer in the interface of NGH dissociation zone and NGH zone.

Laboratory experiments on methane production simulation based on the depressurization have been carried out by many researchers. The experimental reactors with different volumes have also been developed, and in the early studies, the volumes of the most adopted reactors were with 1 L [65-70]. Even recently, the small reactors were extensively used in the experimental studies [13, 71-75]. By the method of depressurization, Yousif et al.[66] simulated the gas production from the hydrates in Berea sandstone cores, and they investigated into the gas production and the position of the hydrate dissociation front as a function of time. Using a 188 mL batch reactor, Kono et al.[71] revealed the methane hydrate dissociation rate somewhat depends on the sediments properties in porous media. In order to validate numerical models of gas hydrate behavior in porous media, Kneafsey et al.[73, 76, 77] performed a series experiments and obtained plenty of valuable experimental data by use of a large X-ray transparent pressure vessel with inner diameter of 76.2 mm and outer diameter of 89.0 mm. Lee et al.[74] built a set of apparatus to analyze the characteristic of hydrate dissociation in porous rocks by depressurization. The main part of the apparatus is a one-dimensional core holder, which allows the fluid flow in axial direction. To account for the naturally occurring sediments in deep sea, the overburden pressure and axial pressure have been applied in addition to the already existing inner pressure of core sample. By depressurizing to 1.93, 0.93 and 0.1 MPa, Tang et al. [78]investigated the gas production from the hydrate-bearing cores. Sun et al.[79] studied methane hydrate dissociation by depressurization at the temperature above 273.15 K and below 273.15 in a sapphire cell. Our group experimentally investigated the effects of pore size, temperature, and initial formation pressure on the dissociation kinetic behaviors of methane hydrates in porous media. In our experiments, the methane production rate and temperature change were also systematically investigated using a one-dimensional with about 280 mL[75]. The conclusions from the experiments were drawn as, on one hand, either the increase of initial pressure or the increase of the mean pore size or the decrease of the environmental temperature has positive effect on the methane production rate, on other hand, the system temperature decreases dramatically during the hydrate dissociation process and then gradually rises to the environmental temperature after it reaches the lowest temperature point. Our conclusion was supported by Haligva et al. [13] who found the initial rate of methane recovery rate is strongly dependent on the silica sand size in the process of methane recovery from a variable-volume bed of silica sand/hydrate by depressurization.

However, to make the experimental simulation of methane production from NGH more consistent with the actual situation and to know more realistic behavior of gas hydrate dissociation, the experimental reactor scale is a crucial factor that should be considered in laboratory experiments. Recently, some hydrate simulation reactors with large volume have been developed. American scientists at Oak Ridge National Laboratory designed a set of Seafloor Process Simulator (SPS) experimental platform with a 72 L reactor to study the gas hydrate dissociation behavior by the method of depressurization [80]. In addition, Zhou et al.[81]developed a set of experimental apparatus with an about 59 L reactor to investigate the methane hydrate dissociation behavior. Chen et al. [82, 83] built a cylindrical experiment device to simulate the behavior of gas hydrate formation and dissociation. The highest operation pressure for the device reaches 16 MPa, and the reactor in the device has an inner diameter of 300 mm and an effective height of 100 mm. The reactor is separated into two parts by a stainless steel board with many pores and 3 mm thickness. The steel board can, thereby, separate porous sediments and free gas during the experiments. There are sixteen thermal resistances distributed in the reactor with different depth and radius for measuring the temperature during the hydrate formation and dissociation. Chen et al.[82, 83] found that the gas production rate changes greatly in different gas production stages by depressurization. In the initial stage, the gas production rate is the fastest. Besides, the initial temperature decreases with the decrease of radius of the reactor. Our team developed a three-dimensional cubic hydrate simulator (CHS) with an effective volume of 5.8 L to study the gas production behavior of methane hydrate in the porous sediments under depressurization [84]. In the CHS, the 25×3 distributed temperature measuring points and 12×3 resistance measuring points were designed. By use of the CHS, the conditions of hydrate reservoir in the Shenhu Area, South China Sea were simulated. And we found the resistances in the hydrate reservoir change with the hydrate dissociation and the flow of the gas and water during the methane production process, and the gas production rate as well as the cumulative gas production increases with the decrease of the pressure. The pressure reduction rate and the heat supplied from the ambient are the two main gating factors for the NGH dissociation. From the scientific simulation view point, the more ideal simulation should be based on the conducted laboratory experiments with a larger reactor to mimic actual field conditions. Nevertheless, to design and develop a reactor with larger volume is rather difficult in practical operation. Moreover, it is quite hard to ensure the synthesized hydrate samples distribute homogeneously in the larger reactor. Till now, a bigger three-dimensional cubic hydrate simulator with volume of 117.8 L has been designed and developed by our team. In the big simulator, which was also called as Pilot-scale Hydrates Simulators (PHS), a 9-spot distribution of vertical wells, a single horizontal well, and 49-spot distribution of thermometers and resistance ports are placed in three horizontal layers, respectively. The schematics of the experimental apparatus and the PHS are shown as in Figures 9 and 10 [25]. Compared with the results obtained from the experiment with the 5.8L CHS [84], the experimental results show the gas production process consists of three periods, such as free gas production, mixed gas production and gas production from hydrate dissociation. The first and second periods are mainly controlled by the pressure reduction rate while the third period is mainly driven by the heat conduction from the ambient. The duration for gas production with the PHS is approximately 20 times as many as that with the CHS during the gas production. Besides, the system temperature change tendency with PHS is the same with that with the CHS while the water production behavior with PHS is different with that with the CHS.

The first production tests using the depressurization method in the world were conducted in the Mallik production program in April 2007 and March 2008[57]. The tests not only successfully attained methane gas from the NGH reservoir, but also revealed the methane recovery highly depends on the reservoir characteristics. Besides, the methane recovery is predicted to be up to 60% even in the favorable case by the tests.

Thermal method

Thermal method means promoting NGH dissociation by increasing temperature of the reservoir. Currently, the general thermal methods include thermal stimulation method and thermal flooding method. The thermal stimulation method aims at increasing the temperature in the vicinity of a well by ways such as hot water circulation, wellbore heating and hot water huff’and puff. The hot water circulation is circulating hot water in a wellbore to increase bottom hole temperature; the wellbore heating is increasing near wellbore temperature by a heater or multi-heaters installed in the down hole; the hot water huff and puff can be described as injecting hot water or steams into the reservoir from a well (huff), then the well is shut-in for a certain period to sufficiently transfer the heat to a reservoir (soak), and then the gas and the water are produced from the same well (puff). The thermal flooding method is depicted as the heat such as hot water or steam is injected from a well and flooded toward other wells increasing temperature, and hence dissociating the NGH between the wells. The detail schematic diagram of the thermal method is shown as picture (b) in Figure 6. For the ways of hot water circulation and wellbore heating, although the NGH dissociation balances the temperature and even the dissociation reduces the temperature in the dissociation region below the three-phase equilibrium temperature, the NGH would dissociate continuously and completely because the heat is continuously supplied. However, because the heat is transferred by thermal conduction, the expansion of the dissociation region with relatively high temperature is extremely slow, resulting in the relatively low gas production efficiency. On the contrary, the ways of hot water huff and puff and hot water flooding induce much faster propagation of the heat and hence much faster expansion of the NGH dissociation areas if the hot water can be injected smoothly. However, because the effective permeability to water is quite low in the presence of NGH with high saturation in the initial stage, it is difficult to keep the hot water injection at high rate. Moreover, the generated natural gas associated the dissociation of NGH near the injection well could be cooled again in the course of the drastic NGH dissociation and reform NGH with free water in the region, which dramatically reduces the permeability and preventing the further smooth injection of hot water[57]. The advantage of the thermal method is that the hydrate decomposition process and the gas production rate could be governed by regulating the amount and the rate of the heat injected. However, from the economic point of view, the method is not suitable for exploitation of hydrates in the permafrost region where the ambient temperature is low and the permafrost layer is thick because the hydrate decomposition is controlled by the thermal characteristics of the hydrate-bearing region.

In 1982, Holder et al.[85] carried the simulation of gas production from a reservoir containing both gas hydrates and free natural gas. In the simulation, they evaluated the feasibility of the thermal method and considered the thermal method is an effective exploitation technology. In addition, McGuire considered the thermal method is quite effective exploitation technology for the hydrate reservoir with high permeability and for a Class 2 hydrate reservoir [86]. In the past decades, many experimental simulations have been carried out using the thermal method [87-89]. Tang et al. [90]investigated into the temperature distribution and flowing characteristics of the dissociated gas and water from hydrates in porous sediments by using a set of one-dimensional experimental apparatus with an internal diameter of 38 mm and a length of 500 mm. They found during the experimental simulation by the thermal method, the higher hydrate content and lower injection temperature and rate, the higher energy ratio. Pang et al.[89] studied the kinetic dissociation behavior of methane hydrate at 268.15K using thermal stimulation method in a closed quiescent middle-sized reactor with inner diameter of 200 mm and length of 320 mm. They found that the rate of heat transfer and the thermodynamic driving force are the key rate-limiting factors for hydrate dissociation in the closed reactor, and the dissociation rate can be increased by increasing the temperature of the heating water and lowering the dissociating pressure. Our team investigated the gas production behavior from methane hydrate in porous sediments by injecting the brine with salinity of 0~24 wt% and the temperature of -1~130℃ in an one-dimensional experimental apparatus[91]. The experimental results show the gas production process consists of three periods, such as the free gas production, the hydrate dissociation, and the general gas reservoir production. The hydrate dissociation accompanies the temperature decease with the injection of the brine, and the dissociation duration shortens while the instantaneous hydrate dissociation rate increase with the increase of the salinity. In addition, we considered the thermal efficiency and energy ratio for the hydrate production can [16]be enhanced by injecting hot brine.

The experimental studies mentioned above were all limited to one or/and two dimensional simulations. Recently, the experimental studies based on three-dimensional simulation were extensively carried out. Yang et al.[92] performed a three-dimensional experimental simulation on gas production from methane hydrate-bearing sand by hot-water cyclic injection. Their experimental results indicated the overall temperature trend increases with hot-water injection but decreases with gas production. The location of the injection/producing well as well as the porosity and permeability of hydrate samples dominate the temperature distribution and fluctuation in the reactor. The energy efficiency ratio is positively impacted by the saturation of the hydrate-bearing sand and temperature but negatively influenced by the hot-water temperature and well pressure in the case of other conditions being similar. Using the CHS, our team devoted ourselves to investigating the methane hydrate production behaviors in porous sediments by the thermal stimulation with a five-spot well system [93]. From the investigation, we found that the hydrate decomposition boundary gradually moves from the central point to the surroundings and finally covers almost the entire hydrate field. The heat conduction plays a more significant role than the convection from the heat diffusion. The increasing injection rate of the hot water enhances the rate of hydrate decomposition, shortens the production time, and decreases the water production volumes. We also found the higher the change of the hot water injection rate (R_{inj}), the higher average production rate and the lower energy efficiency, although the R_{inj} has little influence on the final gas recovery. Based on the experiments with the CHS, we carried out more the experiments with a scale-up reactor which was mentioned as the PHS [94]. The experimental conditions are designed by a set of scaling criteria for gas hydrate reservoir. By the comparison the experiments with the CHS with the experiment with the PHS, we found, on one hand, the gas and water production behaviors are similar, on the other hand, the energy efficiencies for different processes of hydrate decomposition according with the scaling criteria which is proven through the experimental results are identical. And more importantly, the scaling law regulated by the result of the experiments is used for predicting the real-scale hydrate production behavior. For example, in an real-scale hydrate reservoir with the size of 36 m × 36 m × 36 m, methane of 1.168×10^{6} m^{3} in STP is produced after 13.9 days of hydrate production, the gas recovery is 0.73 and the final energy efficiency is 9.5. Beside these work, we also carried out thermal huff and puff experiments by using the CHS and PHS[23, 24, 95-97]. Through the experiments, we systematically investigated the change characteristics of the injection temperature, pressure, resistance ratio and other related parameters during the thermal simulation gas production process. The injected heat spreads out from the injection point, forming a heat flux surface, which enlarges as the number of huff and puff cycles increases, and eventually reaches the surface with the largest impact. Then, the area of the heat flux surface no longer increases with continuous heat injection. In addition, the experimental results also prove that the hydrate decomposition process is a moving boundary ablation process on a three-dimensional level. We also investigated the sensitivities of the hydrate dissociation to the initial hydrate saturation, hot water injection time and hot water initial temperature [96]. The sensitivity analysis indicates the dependence of the gas production on the initial hydrate saturation, and the temperature and the injection rate of the injected hot water. Through the experiments carried out in the PHS, we considered, at a constant hot water injection rate, the range of the thermal diffusion is restricted around the well, and the depressurization is more advantage to the gas production relative to the thermal stimulation [97]. Besides, the experimental results also tell us the gas production efficiency can be improved by prolonging the hot water injection time although the enhancement is limited by the stronger pressurization effect.

The production test using the hot water circulation method was firstly conducted at Mallik site in Canada in 2002. However, since the energy supplied in the thermal method is quite large, the applicability of the method is disputed from the viewpoint of energy efficiency. Recently, scientists generally agree to apply the thermal method as a secondary recovery method after dissociating NGH to some extent by depressurization and making paths for water movement[98].

Inhibitor injection method

For the inhibitor injection method, inhibitors of hydration such as methanol, ethanol, brine, electrolyte solutions, salt and alcohol are injected into a reservoir to shift the three-phase equilibrium conditions to the high pressure and low temperature side, in which the NGH automatically dissociates [99]. However, the shift magnitude is limited, and, the sole inhibitor injection method could not lead to the significant NGH dissociation. Besides, it is difficult to inject the inhibitor smoothly into a reservoir because of the very low initially effective permeability to water. Therefore, the inhibitors are generally injected together with hot water in applying hot water huff and puff or hot water flooding method to improve the energy efficiency. Furthermore, the issues of high cost and dilution/dispersion of inhibitors also limit the application of the inhibitor injection method in gas production.

In addition, the thermodynamic inhibitors can lower the activity of water, making the hydrate formation condition harsher. Therefore, the thermodynamic inhibitors are used to promote the hydrate dissociation and enhance the gas yield in the process of methane production from the hydrate reservoir. Many valuable studies have been reported on the investigation into the gas production in the presence of the inhibitors [99-131]. Through the studies, the hydrate formation equilibrium conditions as well as gas hydrate formation/dissociation behaviors in the presence of inhibitors have been achieved systematically. For volatile inhibitors, Katz et al. [132]found the inhibiting effect reduces with the increase of the volatility of the inhibitors. Beside the volatility, the operating pressure also greatly influences the inhibitor effect. Makogon [133]found, with the increase of pressure, the inhibiting effect reduces first and reaches a minimum, then increases slightly when electrolyte solution ($CaCl_2$) was used as the inhibitor. Sira et al.[125] investigated the hydrate decomposition process by using methanol and ethylene glycol as inhibitors, and they found the hydrate dissociation rate is a function of the concentration of inhibitor, injection rate, pressure, temperature and interfacial area between hydrate and inhibitor. Fan et al. [128] injected 10~30 wt% ethylene glycol into a 3.5 L reactor to investigate the effect of ethylene glycol on methane hydrate dissociation, and they found the hydrate dissociation rate depends on the concentration and the flow rate of ethylene glycol. The similar results were obtained by Li et al.[99]. They injected ethylene glycol into a one-dimensional device to investigate gas production behavior from methane hydrate in porous sediments, and found the production efficiency is affected by the concentration of the ethylene glycol and injection rate. The highest efficiency is achieved when the concentration of the ethylene glycol is 60 wt%. Yuan et al.[131] injected ethylene glycol into a three-dimensional apparatus to investigate gas production behavior from methane-hydrate-bearing sands. They found an optimal value of mass ratio of injected ethylene glycol to initial water exists where a maximum gas production ratio appears. In addition, they found that the concentration of ethylene glycol is positive to either gas production or gas production efficiency, but the gas production efficiency decreases with the increase of the EG quantity.

However, as mentioned above, the inhibitor injection method has not ever been used in field test, because not only the inhibitors are expensive and environment-unfriendly, but also the diffusion of the inhibitors is hindered by the low permeability of hydrate-bearing sediments.

Other methods

Other than the three basic methods introduced above, there are several new methods, which are investigated for producing methane gas from NGH in laboratory. As same as the basic methods, the new methods are also based on shifting the gas-water-NGH three-phase equilibrium conditions to NGH dissociation region. The new methods include gas replacement, ultrasonic wave irradiation, electrical heating and CO_2 injection. Gas replacement is injecting other gas components (e.g. CO_2) into a NGH reservoir to displace methane. Because CO_2 hydrate is generated more easily compared with NGH in the initial methane-water-NGH equilibrium conditions, CH_4 replaced by CO_2 in the hydrates is feasible[35-38]. Furthermore, CO_2 hydrate formation is an exothermal reaction, and the reaction heat further promotes the NGH dissociation after it transfers to the internal NGH deposits by heat conductivity. Ultrasonic wave irradiation method can be briefly described as promoting the dissociation of NGH with vibration of irradiation waves[134]. Electrical heating is based on increasing the reservoir temperature by transmitting the electrical energy such as electrical current or micro wave to a reservoir through electrical probes[135]. Currently, the method of electrical heating is utilized for heavy oil recovery from crude oil. Since CO_2 is the preferred hydrate former below 10 °C relative to CH_4 at pressure lower than 6.5 MPa it is feasibility to spontaneously replace CH_4 in the hydrate without energy introduction[35, 38, 44, 136]. And the method is beneficial because it offers long term storage of CO_2 with the added benefit of produced methane without dissociating the hydrate[137,138]. CO_2 injection mainly include micro-emulsion containing CO_2 injection, dissolved CO_2 injection and pure CO_2 liquid injection[139]. CO_2 injection can shorten the gas production time and reduce the quantity of produced water during the production process, but it also brings potentially detrimental effects to the deep-sea fishes for the permanence of the injected CO_2 changing the pH of the hydrate-bearing region[140].

Among the methods, gas replacement, especially CO_2 replacement, is now studied extensively because of its functions not only in producing CH_4 from NGH but also sequestrating CO_2 directly into sea floor in form of CO_2 hydrate. The studies of CO_2-CH_4 hydrate replacement include thermodynamics, kinetics, molecular dynamics (MD) simulation and experimental simulation. Dissociation enthalpies of CH_4 hydrate and CO_2 hydrate under different conditions of temperature and pressure are systematically obtained through different equations (such as Clapeyron equation, modified Claypeyron equation, Clausius-Clapeyron equation (C-C eq.), modified C-C eq.,thermodynamics equation) and ways (e.g., Calvet heat-flow calorimeter, and Calvet heat-flow differential scanning calorimeter), based on the experimental equilibrium data [141-153].Under the condition of 273.15 K and 3.25 MPa, Gibbs free energy (ΔG) of the reaction of CH_4 replacement by CO_2 in hydrates is about -3.49 kJ/mol , which means the reaction of CO_2 replacing CH_4 from hydrate is a spontaneous reaction[38, 154].The kinetics of CO_2-CH_4 replacement was also extensively studied. In order to qualify and quantify the hydrate formation and dissociation kinetics, many analytical techniques have been proposed, including material balance (MB)[155-164], X-ray diffraction (XRD)[163, 165], neutron diffraction[166], Raman[167-169], nuclear magnetic resonance (NMR)[170-174], magnetic resonance imaging (MRI)[175-177], and particle size analysis (PSA)[157, 178, 179].

At present, two big problems block the application of CO_2 replacement in producing $CH_4$from a NGH reservoir. On one hand, the micro mechanism of the replacement is still not proven; on the other hand, the CH_4 recovery rate and CH_4 replacement efficiency are seriously affected by CO_2 diffusion in a NGH reservoir[180]. In fact, researchers still not confirm what the detail replacement process is. Is it the process that the methane hydrate firstly dissociates and the methane releases from the destructive methane hydrate cavities, and then carbon dioxide hydrate forms? Or is it the process that CO_2 molecules directly replace CH_4 molecules under the condition of keeping the hydrate structure stable? No one has a clear answer. For the governing factor of CO_2-CH_4 replacement rate and efficiency, the mainstream view focuses on the kinetics of methane hydrate dissociation and carbon dioxide hydrate formation, especially on the diffusion of CH_4 or/and CO_2 molecules in the hydrates. However, since the governing factor of the diffusion of gas molecules in the hydrates is confirmed, the researchers have still not proposed any solutions. Thus, the application of CO_2-CH_4 replacement in producing CH_4 from NGH reservoir still has a long way to go.

Molecule dynamics (MD) simulation is one powerful tool to provide molecular level understanding of microscopic mechanisms. Geng et al.[41] investigated the potential of methane reoccupation during replacement of methane hydrate by CO_2 by use of MD simulation. Tung et al.[40] and Qi et al.[181]investigated the microscopic mechanism of CH_4 replacement by CO_2 in the hydrate by use of MD simulations. The force fields models TIP4P-Ew[182] for water, OPLS-AA[183] for methane and EPM2[184] for CO_2 were adopted in the two studies. In Tung et al.'s simulation, a two-phase model consisting of a CO_2 liquid and a solid methane hydrate is used. The CO_2 phase contains 320 CO_2 molecules and the methane hydrate phase consists of a 6×2×2 unit cell of sI hydrate with all its cavities filled with methane (1104 water molecules and 204 CH_4 molecules), and the initial model size is created as 114.00 Å× 23. 74 Å× 23. 74 Å. In Qi et al.'s simulation, 336 three-site CO_2 molecules composes the initial gas phase, and the hydrate phase consists of a 6×2×2 unit cell of sI hydrate with 2944 water molecules and 512 CH_4 molecules. We generally consider that the mechanism of the CO_2-CH_4 replacement in the hydrate should be stable under a certain condition. Tung et al. found the replacement occurs either via (1) directly swapping of methane and CO_2 or via (2) a transient co-occupation of both methane and CO_2 in one cavity. Therefore, they considered that, with a careful design of the operation condition, it is possible to simultaneously recover methane from methane hydrate and sequester CO_2 in the solid phase without much change in the geological stability. But, Qi et al.'s study indicated the replacement process might be described as: the hydrate cages break firstly, then CH_4 molecules run out of the cages, and at the same time, CO_2 molecules enter into the void cages and further form CO_2 hydrates. They also consider that it is necessary to make the hydrate melted once time or increase the interface area to speed up the replacement. It's obvious that the results obtained from the two simulations are not consistent with each other. It is difficult to attribute the different results to the difference of the initial simulation systems in the two simulations, i.e., the setup of the initial simulation system should not be the reason of the different results. Thus, what we can suggest is that, till now, the micro-mechanism of the CO_2-CH_4 replacement in the hydrate is still not clear, and researchers should further investigate how to use MD simulation to draw a consistent conclusion.

Numerical Simulations and Field Production Tests

Numerical Simulations

Numerical simulation is utilized to assess the hydrate production potential for various NGH deposits with different production methods, which are mentioned above and predict the complex system behaviors. It gives specific data for the design of laboratory and field experiments. Over the past 10 years, the numerical simulation has been well developed based on the improved sources of code availability. Currently, there are several numerical models that can simulate the system behavior in NGH deposits. The most commonly used simulators are shown as follows:

(a) The Hydrsim simulator, which is developed by the University of Calcary[185].

(b) The MH 21 code, which is developed by a team including the Japan Oil Engineering Company, the National institute for Advanced Industrial Science and Technology, and the University of Tokyo[186].

(c) The STOMP-HYD code, which is developed by the Pacific Northwest National Laboratory[187].

(d) A hydrate-specific variant of the commercial simulator CMG-STARS[188].

(e) The TOUGH+HYDRATE code, and its earlier version[189, 190].

These simulators are based on the consideration of both fluid flow and heat transfer while the solid phase is assumed to be immobile. Besides, there are other simulators. Kimoto et al.[191] proposed a chemo-thermo-mechanical finite element model to investigate the geo-mechanical effects of hydrate dissociation, and in the model, the effect of convection in the energy conservation equation was ignored. Another geo-mechanical model in FLA2D code was developed by Ng et al.[192] to investigate the wellbore stability during the gas production. In 2008, Rutqvist et al.[193] proposed a numerical method by coupling the simulator TOUGH+HYDRATE with the geo-mechanical code FLAC3D to investigate the coupled thermal, hydraulic and geo-mechanical behaviors of the hydrate reservoirs. In 2009, a fully coupled thermo-hydro-mechanical model was proposed to predict the complex behaviors of NGH reservoirs during the gas production[194]. The model was based on the fully coupled theories of multiple-phase fluid flow, heat transfer and deformation in hydrate media.

However, how to establish a mathematical modeling is a crucial issue to further discuss the prediction of gas production from NGH reservoir. Generally, to develop a mathematical model includes the development of the governing equations, constitutive equations, boundary and initial conditions, and numerical techniques. Meanwhile, in order to reflect the rules of hydrate dissociation, including the flow of gas and liquid, the heat transfer in a multiphase and multiple components in the system, it is necessary to formulate the mass balance equation, the momentum equation, the energy balances, and the mass balances for each component and each phase. For establishing a mathematical modeling, specific phases and components need to be defined in advance. Figure 7 shows a schematic of phases and components in a kinetic model. It is noted that, the phases do not necessarily exist independently. In other words, there can be two phases coexist or three phases coexist. The formulation of the equations is based on series assumption, i.e., (1) hydrate is assumed to be immobile, (2) the flow of gas and fluid in the system follows Darcy's law, (3) the heat transfer is governed by the energy conservation equation including conduction and convection, (4) the equilibrium equation with fast convergence is necessary. The mathematical model generally includes kinetic and equilibrium sub-models. After the establishment of the sub-models, the governing equations for each component and for each phase, thereby, must be confirmed, such as mass balance equation, energy balance equation, momentum equation. For all the equations, the primary variables must be chosen. In general, all these variables are known at time t, and the goal is to calculate these variables at the next time $t+\varDelta t$. Certainly, the choice of the primary variables must follow such principle that other variables occurring in the equations can be expressed as functions of the primary variables. The determination of the governing equations is crucial for establishing the mathematical model. However, the governing equations are not sufficient to fully describe a multiple-phase system, and they must be supplemented with equations that describe the constitutive behavior of the individual phases. At last, it is necessary to determine the boundary and initial conditions, including initial temperature, initial pressure, boundary pressure, size of the simulated zone, initial water saturation, initial gas saturation, initial hydrate saturation, intrinsic permeability, specific heat capacity, porosity, sand thermal conductivity, relative permeability.

Then, a computation domain consisting of a two-dimensional uniform $N\times M$ grid with given $\varDelta x$ and $\varDelta y$ or a three-dimensional uniform $N\times M\times K$ grid with $\varDelta x$, $\varDelta y$ and $\varDelta z$ must be determined for an numerical simulation. In fact, all of the simulations were based on a laboratory-scale experiment[195]. The mesh size is varied in the x, y and z directions until the simulations reach a numerical asymptotic solution with the meshes[196]. The convergence criteria need preset before a numerical simulation and an initial time step are carried out.

Different governing equations used in the numerical calculation determine the features of the correspondingly different simulators and the accuracy of the prediction. Thus, if you want to go for a perfect simulation result, you need carefully consider all kinds of problems as much as possible and adopt variety governing equations into the simulation. It is noted almost all the equations are established based on certain assumptions. However, the certain assumptions may be inconsistent, and the inconsistencies may lead to the equations divergence. That is to say, it is impossible to adopt all equations in a simulation or a simulator. Therefore, almost all the simulators including those mentioned above have their individual shortcomings.

MH21-HYDRES can simulate the CH_4 production by thermal stimulation, depressurization, and/or combination method. It is able to deal with three-dimensional, five-phase, six-component problems. The three-dimensional (3D) Cartesian and two-dimensional (2D) radial coordinates can be applied with local grid refinement. However, to reduce the computational complexity or to cut down the amount of calculation, the meshes used in the simulator are generally coarse. Thereby, it is prone to causing numerical errors. STOMP-HYD is used to reveal the laws of motion and changes of the multi-phase fluids. The hydrate formation and dissociation can be simulated by the STOMP-HYD in the equilibrium models and kinetic models by use of four mass conservation equations and one energy conservation equation. It is noted that hydrates, ice, precipitated salts and guests are assumed as immobile phase[197]. However, the assumption is in contradiction to the realities, for example, the real guests dissociated from the hydrates are mobile. Therefore, the STOMP-HYD simulator has its limitations. The CMG-STARS is specially designed for simulating the flow of multi-component fluids. The TOUGH+HYDRATE can simulate the NGH formation and dissociation with multi-components (including hydrate formation additives) and multi-phases. With the development of simulation technology, TOUGH+ series simulator has gone through different stages, such as TOUGH1, TOUGH2, TOUGH+EOSHYDR, TOUGH-Fx/HYDRATE, TOUGH+HYDRATE. Currently, the TOUGH+HYDRATE becomes the most popular hydrate simulator because more complicated components and phases can be simulated and more accurate results can be obtained [198, 199]. The TOUGH+HYDRATE requires a large number of parameters for support. However, not all the physical parameters are known for a certainly new simulation, and in this case, it is difficult to run the

TOUGH+HYDRATE.

Field Production Tests

Numerical simulation is considered as doing experiments by using computers, and its intentions include index prediction and economic evaluation, new technology evaluation, methane production reveal, potentiality evaluation and development prediction. Based on the different production methods and simulators, a lot of numerical simulations have been carried out, and a lot of valuable simulation results are obtained.

However, the simulation results do not equate to field production. In fact, before the field production or commercial NGH production, there are many problems need overcome[200].The first national NGH program was initiated by Rodney Malone at the U.S. department of Energy research center (now National Energy Technology Laboratory) in Morgantown, West Virginia. The program brought forth a body of work that stimulated others to see NGH as a potential resource that could have economic value rather than as a geochemical oddity [201]. Up to now, NGH has been found in more than 120 sites over the world, but the physical NGH samples were successfully drilled in only two dozen sites. In the aspect of the research of the field NGH production, only 4 drilling tests were carried out, 3 in permafrost regions (Messoyakha hydrate gas field in Western Sibria, Alaska's north slope area, and MacKenzie Delta) and 1 in seafloor (Eastern Nankai Trough, Japan)[202, 203]. Compared to the NGH in the seafloor, the NGH in the permafrost regions can be more easily produced with more simple process. In 1998, the first NGH field production research was carried out by a consortium between the Geological Survey of Canada, the Japan National Oil Corporation, Geo Forschungs Zentrum Potsdam, the U.S. Geological Survey, the U.S. Department of Energy and the Gas Authority of India Ltd/Oil and Natural Gas Corporation Ltd. The Geological Survey of Canada coordinate the science program for the project and JAPEX Canada Ltd is the designated operator for the fieldwork in Mallik gas hydrate field. The Mallik gas hydrate field, located at the northeastern edge of Canada's Mackenzie Delta, occurs within a sequence of Tertiary sediments in an area underlain by over 600m of permafrost. With data obtained from the original discovery well in 1971/72 and a scientific research well program in 1998, gas hydrate occurrences have been well documented. Quantitative well log determinations and core studies reveal at least 10 discrete gas hydrate layers exceed 110 m in total thickness from 890 m to 1106 m depth. High gas hydrate saturation values, which in some cases exceed 80% of the pore volume, determine the Mallik gas hydrate field as one of the most concentrated gas hydrate reservoirs in the world. In the period of December 2001 to March 2002, a production research well program was completed that include drilling of a 1200 m deep main production research well and two nearby science observation wells. Primary objectives of the Mallik 2002 production research well program are to advance fundamental geological, geophysical and geochemical studies of the Mallik gas hydrate field and to undertake advanced production testing of a concentrated gas hydrate reservoir. Full-scale field experiments monitor the physical behavior of the hydrate deposits in response to depressurization and thermal stimulation. The observation wells facilitate cross-hole tomography experiments (before and after production testing) as well as long term monitoring of in situ formation conditions. A wide ranging science and engineering research program include collection of gas-hydrate-bearing core samples and downhole geophysical logging. Laboratory and modeling studies undertaken during the field program, and subsequently as part of a post-field research program document the sedimentology, physical/petrophysical properties, geochemistry, geophysics, reservoir characteristics and production behavior of the Mallik gas hydrate accumulation.

Besides the gas hydrate scientific drillings in the Mallik gas hydrate field, there are many other gas hydrate scientific drillings which have been carried out or will be carried out over the world. Figure 8 shows an outline of international gas hydrate research, including the international gas hydrate research projects and the completed/future gas hydrate scientific drillings[204]. For example, in May of 2007 and June of 2009, Chinese scientists have successfully drilled out NGHs in Shenhu area of South China Sea and Qilianshan Mountain region of China Qinghai-Tibet plateau. The northern slope of the South China Sea is one important area for China to exploit and investigate NGH. According to the report of the China Geological Survey, among the total 8 drilled wells in the South China Sea, the NGH was found in the cores obtained in the three wells (SH2, SH3 and SH7), and core studies revealed the discrete gas hydrate layers with hydrate saturation of 0 ~ 48 % from 1108 m to 1235 m depth, exceeding 40 m in total thickness. It was proven the total NGH distribution area in the Shenhu area of the South China Sea was about 15 km^2 and the methane resource in the NGH was about $1.60\times10^{10}m^3$[205].In the period of 2008 ~ 2009, the Scientific Drilling Project of Natural Gas Hydrate in Qilianshan Mountain Permafrost Region was carried out by the China Geological Survey. In the project, total 4 wells (DK-1, DK-2, DK-3, DK-4) were drilled, and the NGH samples from 133 ~ 396 m depth were obtained in DK-1, DK-2 and DK-3, respectively[206].However, according to the plans made by the China Geological Survey, the field methane production test is not carried out in the above two areas in China until 2016.

Japan is currently leading NGH development. Since 1995, Japan has maintained a focused, well-founded program. This program marked a milestone in March 2013 when about a week technical production test of the 40 TCF Nankai Trough NGH deposit was successfully carried out by JOGMEC. However, we do not consider that the project means the coming of the time of the methane production from the NGH because there are no enough further detail information and data about the project. It was the first technical production test of oceanic NGH according to a planned timeline of JOGMEC[207]. JOGMEC, the Japanese operator, has reaffirmed the aim of the second phase of the Japanese NGH program that is to continually produce natural gas for their home market by 2018. It is a near-term development timeline consistent with the conventional deep water field development. The commercial production of NGH of Japan is likely due to the natural gas produced from the Nankai NGH deposit should compete well with the rather high delivered price of liquefied natural gas (LNG) that has been in the range of ＄15 - ＄18 MMcf in the period of 2011 – 2013. With the improvement of NGH exploration and production techniques, the cost of the exploration and production must decrease gradually, and it is possible that the oceanic NGH may compete on a produced cost with other natural gas resources.

Conclusion

In this paper, we comprehensively review the studies on producing methane from NGH. The NGHs as alternative energy for future extensively distribute oceanic floor and permafrost areas. Among all the NGH reservoirs, the reservoirs of Class 1 are considered to be of exploitation value under the present technique. The reservoirs of Class 2, 3 and 4 are unrecoverable because the reservoir features go against defining gas production targets. The mechanism of methane production from the NGH is based on shifting the condition of the

NGH reservoirs to NGH dissociation. Relative to the other two conventional methods, the depressurization is considered to be the most effective. However, the methane production rate and efficiency by single depressurization are restricted because of the issues such as diffusion and temperature. Thus, the method combined depressurization with thermal stimulation and/or the method combined thermal stimulation with inhibitor injection are developed. The combined method does be benefit to enhance gas production, increase gas production rate and improve the gas production efficiency. The commercial methane production from NGH is still not realized although some field production tests were carried out in Mallik and Nankai Trough, the most important restraint is the issue of the sustainability of the gas production. Till now, no enough information and data prove that the methane production from NGH can be sustainable for more than one month. Therefore, the main studies still focus on the simulations of methane production from NGH. By the simulations, researchers expect to find the key restraints and resolve them. However, there is a lot of work to be done. As a new gas production method, CO_2-CH_4 replacement in NGH attracts many people's eyes for its function of not only recovering CH_4 from NGH but also sequestrating CO_2 directly in the form of CO_2 hydrates. However, the new method also faces the issues of low CH_4 recovery rate and low CH_4 production efficiency. In order to eliminate the issues, it is necessary to confirm the mechanism of the CO_2-CH_4 replacement in NGH and find out the governing factors. Currently, there are some disputes on the mechanism. MD simulation is a good way to resolve the disputes. MD simulation helps to reveal the CO_2-CH_4 replacement process in molecular level. But, how to construct a MD simulation model becomes a crucial problem because the difference models can lead to different results.

Acknowledgments

This work was supported by the National Science Foundation for Distinguished Young Scholars of China (51225603), and the National Natural Science Foundation of China (51376184, 51476174). We gratefully acknowledge each of these supporting agencies.

References

1. K. A. Kvenvolden, *Rev Geophys*, 1993, 31, 173-187.
2. K. A. Kvenvolden, G. D. Ginsburg and V. A. Soloviev, *Geo-Mar Lett*, 1993, 13, 32-40.
3. V. Gornitz and I. Fung, *Global Biogeochem Cy*, 1994, 8, 335-347.
4. D. Archer, B. Buffett and V. Brovkin, *P Natl Acad Sci USA*, 2009, 106, 20596-20601.
5. E. B. Burwicz, L. H. Rupke and K. Wallmann, *Geochim Cosmochim Ac*, 2011, 75, 4562-4576.
6. , *Realizingthe Energy Potential of MethaneHydratefor the United States*, The NATIONAL ACADEMIES PRESS, Washington, D.C., 2010.
7. P. Englezos, *Ind Eng Chem Res*, 1993, 32, 1251-1274.
8. G. J. Moridis, T. S. Collett, S. R. Dallimore, T. Satoh, S. Hancock and B. Weatherill, *J Petrol Sci Eng*, 2004, 43, 219-238.
9. G. J. Moridis, T. S. Collett, R. Boswell, M. Kurihara, M. T. Reagan, C. Koh and E. D. Sloan, *Spe Reserv Eval Eng*, 2009, 12, 745-771.
10. S. A. Bagherzadeh, S. Alavi, J. A. Ripmeester and P. Englezos, *Fluid Phase Equilibr*, 2013, 358, 114-120.
11. S. A. Bagherzadeh, P. Englezos, S. Alavi and J. A. Ripmeester, *J Phys Chem B*, 2012, 116, 3188-3197.
12. S. A. Bagherzadeh, P. Englezos, S. Alavi and J. A. Ripmeester, *J Chem Thermodyn*, 2012, 44, 13-19.
13. C. Haligva, P. Linga, J. A. Ripmeester and P. Englezos, *Energ Fuel*, 2010, 24, 2947-2955.
14. S. Alavi and J. A. Ripmeester, *J Chem Phys*, 2010, 132.
15. S. Y. Lee and G. D. Holder, *Fuel Process Technol*, 2001, 71, 181-186.
16. G. J. Moridis and T. S. Collett, *Advances in the Study of Gas Hydrates*, 2004, DOI: Doi 10.1007/0-306-48645-8_6, 83-97.
17. G. J. Moridis, *Spe Reserv Eval Eng*, 2004, 7, 175-183.
18. G. J. Moridis and M. T. Reagan, *J Petrol Sci Eng*, 2011, 76, 124-137.
19. G. J. Moridis and E. D. Sloan, *Energ Convers Manage*, 2007, 48, 1834-1849.
20. A. Demirbas, *Energ Convers Manage*, 2010, 51, 1562-1571.
21. G. Ahmadi, C. A. Ji and D. H. Smith, *Energ Convers Manage*, 2007, 48, 2053-2068.
22. N. Goel, M. Wiggins and S. Shah, *J Petrol Sci Eng*, 2001, 29, 115-127.
23. X. S. Li, Y. Wang, L. P. Duan, G. Li, Y. Zhang, N. S. Huang and D. F. Chen, *Appl Energ*, 2012, 94, 48-57.
24. B. Li, G. Li, X. S. Li, Q. P. Li, B. Yang, Y. Zhang and Z. Y. Chen, *Energ Fuel*, 2012, 26, 7183-7194.
25. Y. Wang, X. S. Li, G. Li, J. C. Feng, Z. Y. Chen and Y. Zhang, Beijing, China, 2014.
26. O. Urdahl, A. Lund, P. Mork and T. N. Nilsen, *Chem Eng Sci*, 1995, 50, 863-870.
27. N. Daraboina, C. Malmos and N. von Solms, *Fuel*, 2013, 108, 749-757.
28. A. Lund, O. Urdahl and S. S. Kirkhorn, *Chem Eng Sci*, 1996, 51, 3449-3458.
29. P. Engelzos, *Proceedings of the Fifth (1995) International Offshore and Polar Engineering Conference, Vol I*, 1995, 289-296.
30. C. C. Gryte, *Ann Ny Acad Sci*, 1994, 715, 323-329.
31. K. Ohgaki, K. Takano, H. Sangawa, T. Matsubara and S. Nakano, *J Chem Eng Jpn*, 1996, 29, 478-483.
32. S. Hirohama, Y. Shimoyama, A. Wakabayashi, S. Tatsuta and N. Nishida, *J Chem Eng Jpn*, 1996, 29, 1014-1020.

33. T. Komai and Y. Yamamoto, *Abstr Pap Am Chem S*, 1997, 213, 90-Fuel.
34. S. Nakano, K. Yamamoto and K. Ohgaki, *P I Mech Eng a-J Pow*, 1998, 212, 159-163.
35. X. T. Zhou, S. S. Fan, D. Q. Liang and J. W. Du, *Energ Convers Manage*, 2008, 49, 2124-2129.
36. T. Uchida, I. Y. Ikeda, S. Takeya, Y. Kamata, R. Ohmura, J. Nagao, O. Y. Zatsepina and B. A. Buffett, *Chemphyschem*, 2005, 6, 646-654.
37. R. Anderson, M. Llamedo, B. Tohidi and R. W. Burgass, *J Phys Chem B*, 2003, 107, 3507-3514.
38. M. Ota, Y. Abe, M. Watanabe, R. L. Smith and H. Inomata, *Fluid Phase Equilibr*, 2005, 228, 553-559.
39. C. G. Xu, X. S. Li, J. Cai, Z. Y. Chen and C. Chen, *CIESC Jounal*, 2013, 64, 7.
40. Y. T. Tung, L. J. Chen, Y. P. Chen and S. T. Lin, *J Phys Chem B*, 2011, 115, 15295-15302.
41. C. Y. Geng, H. Wen and H. Zhou, *J Phys Chem A*, 2009, 113, 5463-5469.
42. Y. Iwai, H. Nakamura and M. Hirata, *Mol Simulat*, 2012, 38, 481-490.
43. K. F. Yan, X. S. Li, Z. Y. Chen and C. G. Xu, *Acta Phys Sin-Ch Ed*, 2010, 59, 4313-4321.
44. M. Ota, K. Morohashi, Y. Abe, M. Watanabe, R. L. Smith and H. Inomata, *Energ Convers Manage*, 2005, 46, 1680-1691.
45. J. B. Wang, X. Q. Guo, G. J. Chen, Z. Z. Li and L. Y. Yang, *J. Chem. Eng. Chin. Univ*, 2007, 21, 5.
46. H. Lee, Y. Seo, Y. T. Seo, I. L. Moudrakovski and J. A. Ripmeester, *Angew Chem Int Edit*, 2003, 42, 5048-5051.
47. L. J. Xiong, X. S. Li, Z. Y. Zeng, G. Li, Z. Y. Chen, Y. Zhang and Q. P. Li, presented in part at the Proceedings of the 7th International Conference on Gas Hydrate (ICGH), Edinburgh, UK, July 17-21, 2011.
48. Q. Yuan, C. Y. Sun, B. Liu, X. Wang, Z. W. Ma, Q. L. Ma, L. Y. Yang, G. J. Chen, Q. P. Li, S. Li and K. Zhang, *Energ Convers Manage*, 2013, 67, 8.
49. X. T. Zhou, S. S. Fan, D. Q. Liang and J. W. Du, *Energ Fuel*, 2008, 22, 1759-1764.
50. W. Zhang, Z. Wang, W. Q. Li, W. Y. Li and D. W. He, *Nat. Gas Chem. Eng.*, 2009, 34, 5.
51. B. P. McGrail, T. Zhu, R. B. Hunter, M. D. White, S. L. Patil and A. S. Kulkarni, presented in part at the Proceedings of the AAPG Hedberg Conference on Gas Hydrates: Engergy Resource Potential and Associated Geologic Hazards, Vancouver, Canada, Sep 12-16, 2004.
52. K. Yamamoto and S. Dallimore, in *Fire in the Ice*, National EnergyTechnologyLaborary, vol. 8, p. 20.
53. Japan extracts gas from methane hydrate in world first, http://www.bbc.co.uk/news/business-21752441, Accessed 13 March, 2013.
54. R. Boswell, Natural Gas Hydrates, http://www.nmsfocean.org/files/6.2_RayBoswell.pdf.
55. R. Boswell, R. Hunter, T. S. Collett, S. Digert, S. Hancock, M. Weeks and M. E. S. Team, Vancouver, Canada, 2008.
56. H. Takahashi and Y. Tsuji, Houston, Texas, USA, 2005.
57. M. Numasawa, S. R. Dallimore, K. Yamamoto, M. Yasuda, Y. Imasato, T. Mizuta, M. Kurihara, Y. Masuda, T. Fujii, K. Fujii, J. F. Wright, F. M. Nixon, B. Cho, T. Ikegami and H. Sugiyama, Vancouver, Canada, 2008.
58. R. Boswell and T. Collett, USDepartment of Energy, Office of Fossil Energy, National Energy Technology Laboratory, 2006, vol. 6(3), pp. 5-7.

59. G. Moridis and T. Collett, presented in part at the TOUGH Symposium, Berkeley, CA, May 12-14, 2003.

60. M. Kurihara and H. Narita, Edingburgh, Scotland, United Kingdom, 2011.

61. G. J. Moridis, T. S. Collett, M. Pooladi-Darvish, S. Hancock, C. Santamarina, R. Boswell, T. Kneafsey, J. Rutqvist, M. B. Kowalsky, M. T. Reagan, E. D. Sloan, A. K. Sum and C. A. Koh, *Spe Reserv Eval Eng*, 2011, 14, 76-112.

62. Q. Yuan, C. Y. Sun, B. Liu, X. Wang, Z. W. Ma, Q. L. Ma, L. Y. Yang, G. J. Chen, Q. P. Li, S. Li and K. Zhang, *Energ Convers Manage*, 2013, 67, 257-264.

63. K. Tsuyuki, S. Tokaji, S. Miura, H. Fujimura and D. Tajima, *Journal of the Jananese Association for Petroleum Technology*, 2009, 74, 6.

64. H. Minagawa, T. Ito, S. Kimura, H. Kaneko and H. Narita, *Int J Offshore Polar*, 2014, 24, 218-223.

65. E. D. Sloan, ed., *Clathrate Hydrates of Natural Gases*, *Third Edition*, CRC Press, Golden, Colorado, U.S.A, 2008.

66. M. H. Yousif, P. M. Li, M. S. Selim and E. D. Sloan, *J Inclus Phenom Mol*, 1990, 8, 71-88.

67. M. H. Yousif, H. H. Abass, M. S. Selim and E. D. Sloan, *Spe Reserv Eval Eng*, 1991, 6, 7.

68. D. W. Davidson, S. K. Garg, C. I. Ratcliffe, J. S. Tse and S. R. Gough, *Can J Chem*, 1984, 62, 1229-1235.

69. V. T. John and G. D. Holder, *J Chem Eng Data*, 1982, 27, 18-21.

70. M. W. C. Dharmawardana, *J Phys Chem-Us*, 1983, 87, 4185-4190.

71. H. O. Kono, S. Narasimhan, F. Song and D. H. Smith, *Powder Technol*, 2002, 122, 239-246.

72. L. G. Tang, X. S. Li, Z. P. Feng, G. Li and S. S. Fan, *Energ Fuel*, 2007, 21, 227-233.

73. T. J. Kneafsey, L. Tomutsa, G. J. Moridis, Y. Seol, B. M. Freifeld, C. E. Taylor and A. Gupta, *J Petrol Sci Eng*, 2007, 56, 108-126.

74. J. Lee, S. Park and W. Sung, *Energ Convers Manage*, 2010, 51, 2510-2515.

75. X. S. Li and Y. Zhang, *Ind Eng Chem Res*, 2011, 50, 8263-8271.

76. T. J. Kneafsey, L. Tomutsa, C. Taylor, A. Gupta, G. J. Moridis, B. Freifeld and Y. Seol, *Abstr Pap Am Chem S*, 2005, 229, U592-U592.

77. T. J. Kneafsey, H. L. Lu, W. Winters, R. Boswell, R. Hunter and T. S. Collett, *Mar Petrol Geol*, 2011, 28, 381-393.

78. C. Y. Sun and G. J. Chen, *Fluid Phase Equilibr*, 2006, 242, 123-128.

79. X. Sun, N. Nanchary and K. K. Mohanty, *Transport Porous Med*, 2005, 58, 315-338.

80. T. J. Phelps, D. J. Peters, S. L. Marshall, O. R. West, L. Y. Liang, J. G. Blencoe, V. Alexiades, G. K. Jacobs, M. T. Naney and J. L. Heck, *Rev Sci Instrum*, 2001, 72, 1514-1521.

81. Y. Zhou, M. J. Castaldi and T. M. Yegulalp, *Ind Eng Chem Res*, 2009, 48, 3142-3149.

82. K. H. Su, C. Y. Sun, X. Yang, G. J. Chen and S. S. Fan, *J Nat Gas Chem*, 2010, 19, 210-216.

83. X. Yang, C. Y. Sun, K. H. Su, Q. Yuan, Q. P. Li and G. J. Chen, *Energ Convers Manage*, 2012, 56, 1-7.

84. X. S. Li, Y. Zhang, G. Li, Z. Y. Chen and H. J. Wu, *Energ Fuel*, 2011, 25, 4497-4505.

85. G. D. Holder, P. F. Angert and S. P. Godbole, New Orleans, LA, USA, 1982.

86. P. L. McGuire, Calgary, Canada, 1981.

87. V. A. Kamath and G. D. Holder, *Aiche J*, 1987, 33, 347-350.

88. J. W. Ullerich, M. S. Selim and E. D. Sloan, *Aiche J*, 1987, 33, 747-752.

89. W. X. Pang, W. Y. Xu, C. Y. Sun, C. L. Zhang and G. J. Chen, *Fuel*, 2009, 88, 497-503.

90. L. G. Tang, R. Xiao, C. Huang, Z. P. Feng and S. S. Fan, *Energ Fuel*, 2005, 19, 2402-2407.
91. X. S. Li, L. H. Wan, G. Li, Q. P. Li, Z. Y. Chen and K. F. Yan, *Ind Eng Chem Res*, 2008, 47, 9696-9702.
92. X. Yang, C. Y. Sun, Q. Yuan, P. C. Ma and G. J. Chen, *Energ Fuel*, 2010, 24, 5912-5920.
93. Y. Wang, X. S. Li, G. Li, Y. Zhang, B. Li and Z. Y. Chen, *Appl Energ*, 2013, 110, 90-97.
94. Y. Wang, X. S. Li, G. Li, Y. Zhang and J. C. Feng, *Appl Energ*, 2014, 115, 47-56.
95. X. S. Li, Y. Wang, G. Li, Y. Zhang and Z. Y. Chen, *Energ Fuel*, 2011, 25, 1650-1658.
96. G. Li, X. S. Li, Y. Wang and Y. Zhang, *Energy*, 2011, 36, 3170-3178.
97. X. S. Li, B. Yang, G. Li, B. Li, Y. Zhang and Z. Y. Chen, *Fuel*, 2012, 94, 486-494.
98. M. Kurihara, A. Sato, H. Ouchi, H. Narita, Y. Masuda, T. Saeki and T. Fujii, *Spe Reserv Eval Eng*, 2009, 12, 477-499.
99. G. Li, X. S. Li, L. G. Tang and Y. Zhang, *Energ Fuel*, 2007, 21, 3388-3393.
100. M. J. Ross and L. S. Toczylkin, *J Chem Eng Data*, 1992, 37, 488-491.
101. A. H. Mohammadi and D. Richon, *J Chem Eng Data*, 2011, 56, 4544-4548.
102. P. Servio and P. Englezos, *J Chem Eng Data*, 1997, 42, 800-801.
103. P. Englezos and P. R. Bishnoi, *Aiche J*, 1988, 34, 1718-1721.
104. P. Englezos, Z. Huang and P. R. Bishnoi, *J Can Petrol Technol*, 1991, 30, 148-155.
105. U. Hutz and P. Englezos, *Fluid Phase Equilibr*, 1996, 117, 178-185.
106. Z. Atik, C. Windmeier and L. R. Oellrich, *J Chem Eng Data*, 2006, 51, 1862-1867.
107. A. H. Mohammadi and D. Richon, *Ind Eng Chem Res*, 2006, 45, 8207-8212.
108. H. Najibi, A. H. Mohammadi and B. Tohidi, *Ind Eng Chem Res*, 2006, 45, 4441-4446.
109. A. H. Mohammadi and D. Richon, *Ind Eng Chem Res*, 2006, 45, 8154-8157.
110. A. H. Mohammadi and D. Richon, *Ind Eng Chem Res*, 2007, 46, 3852-3857.
111. A. H. Mohammadi and D. Richon, *Ind Eng Chem Res*, 2007, 46, 987-989.
112. A. H. Mohammadi and D. Richon, *Ind Eng Chem Res*, 2010, 49, 8865-8869.
113. A. H. Mohammadi and D. Richon, *J Chem Thermodyn*, 2012, 44, 26-30.
114. A. H. Mohammadi and D. Richon, *J Chem Thermodyn*, 2012, 53, 82-85.
115. J. Javanmardi, S. Babaee, A. Eslamimanesh and A. H. Mohammadi, *J Chem Eng Data*, 2012, 57, 1474-1479.
116. K. N. Mahadev and P. R. Bishnoi, *Can J Chem Eng*, 1999, 77, 718-722.
117. P. R. Bishnoi and P. D. Dholabhai, *Fluid Phase Equilibr*, 1999, 160, 821-827.
118. P. D. Dholabhai, J. S. Parent and P. R. Bishnoi, *Fluid Phase Equilibr*, 1997, 141, 235-246.
119. A. H. Mohammadi, W. Aftal and D. Richon, *J Chem Eng Data*, 2008, 53, 73-76.
120. A. H. Mohammadi, W. Afzal and D. Richon, *J Chem Eng Data*, 2008, 53, 683-686.
121. W. Afzal, A. H. Mohammadi and D. Richon, *J Chem Eng Data*, 2008, 53, 663-666.
122. A. H. Mohammadi, I. Kraouti and D. Richon, *Ind Eng Chem Res*, 2008, 47, 8492-8495.
123. A. H. Mohammadi, S. Laurens and D. Richon, *J Chem Eng Data*, 2009, 54, 3118-3120.
124. A. Elgibaly and A. Elkamel, *Energ Fuel*, 1999, 13, 105-113.
125. J. H. Sira, S. L. Patil and V. A. Kamath, New Orleans, LA, USA, 1990.
126. T. Kawamura, Y. Sakamoto, M. Ohtake, Y. Yamamoto, T. Komai, H. Haneda and J. H. Yoon, *Ind Eng Chem Res*, 2006, 45, 360-364.
127. T. Kawamura, Y. Sakamoto, M. Ohtake, Y. Yamamoto, H. Haneda, J. H. Yoon and T. Komai, *Int J Offshore Polar*, 2006, 16, 5-9.
128. S. S. Fan, Y. Z. Zhang, G. L. Tian, D. Q. Liang and D. L. Li, *Energ Fuel*, 2006, 20, 324-326.

129. F. H. Dong, X. Y. Zang, D. L. Li, S. A. S. Fan and D. Q. Liang, *Energ Fuel*, 2009, 23, 1563-1567.
130. J. Lee, *Energ Fuel*, 2010, 24, 456-463.
131. Q. Yuan, C. Y. Sun, X. Yang, P. C. Ma, Z. W. Ma, Q. P. Li and G. J. Chen, *Energ Fuel*, 2011, 25, 3108-3115.
132. D. L. Katz, D. Cornell, F. H. Poettmann, J. A. Vary and J. R. Elenbaas, eds., *Handbook of Natural Gas Engineering*, McGraw-Hill Book Inc., New York, NY, USA, 1959.
133. Y. F. Makogon, ed., *Hydrates of Natural Gas*, PennWell, Tulsa, OK, USA, 1981.
134. K. Tsuyuki, S. Tokaji, S. Miura, H. Fujimura and D. Tajima, *Journal of the JananeseAssociationfor Petroleum Technology*, 2009, 74, 6.
135. H. Minagawa, Y. Nishikawa, Y. Takahashi and H. Narita, presented in part at the Eighth ISOPE Ocean Mining Symposium, Chennai, India, 20-24 September, 2009.
136. M. Ota, T. Saito, T. Aida, M. Watanabe, Y. Sato, R. L. Smith and H. Inomata, *Aiche J*, 2007, 53, 2715-2721.
137. C. Hågenvik, Master, University of Bergen Norway, 2013.
138. Y. Ikegawa, T. Ebinuma, K. Suzuki, Y. Masuda, H. Narita and K. Miyakawa, presented in part at the The Offshore Technology Conference, Houston, Texas, 2010.
139. M. White and P. McGrail, *Greenhouse Gas Control Technologies 9*, 2009, 1, 3099-3106.
140. A. Ishimatsu, Y. Kojima and M. Hayashi, in *Nagasaki University's Academic Output SITE*, IEEE, 2008, ch. 1, p. 4.
141. R. Anderson, M. Llamedo, B. Tohidi and R. W. Burgass, *J Phys Chem B*, 2003, 107, 3500-3506.
142. P. Skovborg and P. Rasmussen, *Fluid Phase Equilibr*, 1994, 96, 223-231.
143. E. D. Sloan and F. Fleyfel, *Fluid Phase Equilibr*, 1994, 96, 233-235.
144. A. Gupta, J. Lachance, E. D. Sloan and C. A. Koh, *Chem Eng Sci*, 2008, 63, 5848-5853.
145. T. Uchida, T. Ebinuma and T. Ishizaki, *J Phys Chem B*, 1999, 103, 3659-3662.
146. K. Seshadri, J. W. Wilder and D. H. Smith, *J Phys Chem B*, 2001, 105, 2627-2631.
147. Y. P. Handa and D. Stupin, *J Phys Chem-Us*, 1992, 96, 8599-8603.
148. S. P. Kang, H. Lee and B. J. Ryu, *J Chem Thermodyn*, 2001, 33, 513-521.
149. J. H. Yoon, Y. Yamamoto, T. Komai, H. Haneda and T. Kawamura, *Ind Eng Chem Res*, 2003, 42, 1111-1114.
150. D. N. Glew, *Can J Chem*, 2002, 80, 418-439.
151. M. B. Rydzy, J. M. Schicks, R. Naumann and J. Erzinger, *J Phys Chem B*, 2007, 111, 9539-9545.
152. G. K. Anderson, *J Chem Thermodyn*, 2003, 35, 1171-1183.
153. K. Ohgaki, Y. Makihara and K. Takano, *J Chem Eng Jpn*, 1993, 26, 558-564.
154. P. Dornan, S. Alavi and T. K. Woo, *J Chem Phys*, 2007, 127.
155. S. Bergeron and P. Servio, *Aiche J*, 2008, 54, 2964-2970.
156. M. Clarke and P. R. Bishnoi, *Can J Chem Eng*, 2001, 79, 143-147.
157. M. A. Clarke and P. R. Bishnoi, *Chem Eng Sci*, 2004, 59, 2983-2993.
158. S. P. Kang and J. W. Lee, *Chem Eng Sci*, 2010, 65, 1840-1845.
159. T. Komai, S. P. Kang, J. H. Yoon, Y. Yamamoto, T. Kawamura and M. Ohtake, *J Phys Chem B*, 2004, 108, 8062-8068.
160. J. W. Lee, M. K. Chun, K. M. Lee, Y. J. Kim and H. Lee, *Korean J Chem Eng*, 2002, 19,

673-678.
161. M. Y. Liang, G. J. Chen, C. Y. Sun, L. J. Yan, J. Liu and Q. L. Ma, *J Phys Chem B*, 2005, 109, 19034-19041.
162. M. B. Malegaonkar, P. D. Dholabhai and P. R. Bishnoi, *Can J Chem Eng*, 1997, 75, 1090-1099.
163. S. Takeya, T. Hondoh and T. Uchida, *Gas Hydrates: Challenges for the Future*, 2000, 912, 973-982.
164. B. Kvamme, A. Graue, E. Aspenes, T. Kuznetsova, L. Granasy, G. Toth, T. Pusztai and G. Tegze, *Phys Chem Chem Phys*, 2004, 6, 2327-2334.
165. C. C. Tang, M. C. Miller, R. J. Cernik, S. M. Clark, C. A. Koh, R. E. Motie, R. I. Nooney, R. Westacott, R. Wisbey and J. L. Savidge, *Epdic 5, Pts 1 and 2*, 1998, 278-2, 335-340.
166. R. W. Henning, A. J. Schultz, V. Thieu and Y. Halpern, *J Phys Chem A*, 2000, 104, 5066-5071.
167. T. Komai, T. Kawamura, S. Kang, K. Nagashima and Y. Yamamoto, *J Phys-Condens Mat*, 2002, 14, 11395-11400.
168. R. Susilo, J. A. Ripmeester and P. Englezos, *Chem Eng Sci*, 2007, 62, 3930-3939.
169. E. D. Sloan, *Fundamentals of Advanced Materials for Energy Conversion*, 2002, 209-226
829.
170. S. P. Kang, H. J. Ryu and Y. Seo, *Proc Wrld Acad Sci E*, 2007, 22, 421-426.
171. J. A. Ripmeester, R. Susilo and P. Englezos, *Chem Eng Sci*, 2007, 62, 3930-3939.
172. Y. Seo and S. P. Kang, *Chem Eng J*, 2010, 161, 308-312.
173. A. K. Sum, R. C. Burruss and E. D. Sloan, *J Phys Chem B*, 1997, 101, 7371-7377.
174. H. H. Lee, S. H. Ahn, B. U. Nam, B. S. Kim, G. W. Lee, D. Moon, H. J. Shin, K. W. Han and J. H. Yoon, *Environ Sci Technol*, 2012, 46, 4184-4190.
175. B. Kvamme, A. Graue, T. Buanes, T. Kumetsoua and G. Ersland, *Int J Greenh Gas Con*, 2007, 1, 236-246.
176. G. Ersland, J. Husebo, A. Graue and B. Kvamme, *Greenhouse Gas Control Technologies 9*, 2009, 1, 3477-3484.
177. G. Ersland, J. Husebo, A. Graue, B. A. Baldwin, J. Howard and J. Stevens, *Chem Eng J*, 2010, 158, 25-31.
178. M. A. Clarke and P. R. Bishnoi, *Chem Eng Sci*, 2005, 60, 695-709.
179. M. Clarke and P. R. Bishnoi, *Gas Hydrates: Challenges for the Future*, 2000, 912, 556-563.
180. D. Y. Koh, H. Kang, D. O. Kim, J. Park, M. Cha and H. Lee, *Chemsuschem*, 2012, 5, 1443-1448.
181. Y. X. Qi, M. Ota and H. Zhang, *Energ Convers Manage*, 2011, 52, 2682-2687.
182. W. L. Jorgensen, J. Chandrasekhar, J. D. Madura, R. W. Impey and M. L. Klein, *J Chem Phys*, 1983, 79, 926-935.
183. W. L. Jorgensen, D. S. Maxwell and J. TiradoRives, *J Am Chem Soc*, 1996, 118, 11225-11236.
184. J. G. Harris and K. H. Yung, *J Phys Chem-Us*, 1995, 99, 12021-12024.
185. H. Hong and M. Pooladi-Darvish, *J Can Petrol Technol*, 2005, 44, 39-46.
186. M. Kurihara, K. Funatsu, H. Ouchi, Y. Masuda and H. Narita, Trondheim, Norway, 2005.
187. H. A. Phale, T. Zhu, M. D. White and B. P. McGrail, Calgary, Albert, Canada, 2006.
188. C. M. Group.
189. G. J. Moridis, M. B. Kowalsky and K. Pruess, *TOUGH-Fx/HYDRATE v1.0 User's Manual: A Code for the Simulation of System Behavior in Hydrate-Bearing Geologic Media*, Lawrence

Berkeley National Laboratory, Berkely, CA, 2005.

190. N. E. T. Laboratory, The National Methane Hydrates R&D Program, Hydrate Modeling - TOUGH-Fx/HYDRATE & HydrateResSim, http://www.netl.doe.gov/technologies/oil-gas/FutureSupply/MethaneHydrates/rdprogram/ToughFX/ToughFx.html#HydrateResSim.
191. S. Kimoto, F. Oka, T. Fushita and M. Fujiwaki, *Comput Geotech*, 2007, 34, 216-228.
192. M. Y. Ng, A. Klar and K. Soga, presented in part at the Offshore Technology Conference, Houston, Texas, U.S.A., 2008.
193. J. Rutqvist, G. J. Moridis, T. Grover and T. Collett, *J Petrol Sci Eng*, 2009, 67, 1-12.
194. H. L. Fang, Hangzhou, China, 2009.
195. Y. Masuda, Y. Fujinaga, S. Naganawa, K. Fujita, k. Sato and Y. Hayashi, Salt Lake City, Utah, USA, 1999.
196. I. K. Gamwo and Y. Liu, *Ind Eng Chem Res*, 2010, 49, 5231-5245.
197. M. D. White and M. Oostrom, *Subsurface transport over multiple phases application guide*, Pacific Northwest National Laboratory, Washington, USA, 1997.
198. G. J. Moridis, M. B. Kowalsky and K. Pruess, *TOUGH+HYDRATE user's manual: A code for the simulation of system behavior in hydrate-bearing geologic media*, Lawrence Berkeley National Laboratory, Berkeley, USA, 2008.
199. K. N. Zhang, G. J. Moridis and Y. S. Wu, Vancouver, Canada, 2008.
200. I. Durgut and M. Parlaktuna, *Ngh '96 - 2nd International Conference on Natural Gas Hydrates, Proceedings*, 1996, 549-556.
201. M. D. Max, A. H. Johnson and W. P. Dillon, Springer, 2013, DOI: 10.1007/978-3-319-02508-7.
202. V. A. Kamath, *A Perspective on Gas Production from Hydrate*, The JNOC's Methane Hydrate International Symposium, Chiba, Japan, 1998.
203. S. R. Dallimore and T. s. Collett, *Summary and Implications of the Mallik 2002 Gas Hydrate Production Research Well Program*, Geological Survey of Canada, Ottawa, Canada, 2005.
204. T. S. Collett, International Gas Hydrate Research - March 2014, http://energy.gov/sites/prod/files/2014/04/f14/International_Review_USGS_Collett%5B1%5D.pdf, Accessed 14 April, 2014, 2014.
205. X. K. Ruan, M. J. Yang, Y. H. Li, Y. C. Song and H. F. Liang, *Natural Gas Exploration & Development*, 2012, 35, 5.
206. Y. H. Zhu, Y. Q. Zhang, H. J. Wen, Z. Q. Lu and P. K. Wang, *Acta Geoscientica Sinica*, 2010, 31, 10.
207. M. Kurihara, H. Ouchi, A. Sato, K. Yamamoto, S. Noguchi, J. Narita, N. Nagao and Y. Masuda, Edinburgh, Scotland, United Kingdom, 2011.
208. S. H. Hancock, G. J. Moridis, A. Robertson and S. Wilson, presented in part at the Offshore Technology Conference, Houston, Texas, USA, 2010.
209. B. Li, X. S. Li, G. Li, J. C. Feng and Y. Wang, *Appl Energ*, 2014, 129, 274-286.
210. A. Shahbazi and M. Pooladi-Darvish, *Spe J*, 2014, 19, 191-205.
211. A. Chejara, B. Kvamme, M. T. Vafaei and K. Jemai, *Energ Convers Manage*, 2013, 68, 313-323.
212. S. Falser, S. Uchida, A. C. Palmer, K. Soga and T. S. Tan, *Energ Fuel*, 2012, 26, 6259-6267.
213. J. C. Feng, G. Li, X. S. Li, B. Li and Z. Y. Chen, *Energies*, 2013, 6, 5402-5425.

214. G. C. Fitzgerald and M. J. Castaldi, *Ind Eng Chem Res*, 2013, 52, 6571-6581.
215. C. Ji, G. Ahmadi and D. H. Smith, *Chem Eng Sci*, 2001, 56, 5801-5814.
216. X. X. Jiang, S. X. Li and L. N. Zhang, *Energy*, 2012, 39, 281-285.
217. T. Kawamura, M. Ohtake, Y. Sakamoto, Y. Yamamoto, H. Haneda, T. Komai and S. Higuchi, *Proceedings of the Seventh (2007) Isope Ocean Mining (& Gas Hydrates) Symposium*, 2007, 83-86.
218. T. Kawamura, M. Ohtake, Y. Yamamoto, H. Haneda, Y. Sakamoto and T. Komai, *Int J Offshore Polar*, 2010, 20, 125-131.
219. T. Kawamura, Y. Yamamoto, M. Ohtake, Y. Sakamoto, H. Haneda and T. Komai, *Proceedings of the Sixth (2005) ISOPE Ocean Mining Symposium*, 2005, 208-212.
220. J. H. Kim, M. E. Torres, J. Y. Lee, W. L. Hong, M. Holland, M. H. Park, J. Choi and G. Y. Kim, *Org Geochem*, 2013, 62, 86-95.
221. Y. Konno, Y. Masuda, Y. Hariguchi, M. Kurihara and H. Ouchi, *Energ Fuel*, 2010, 24, 1736-1744.
222. G. Li, B. Li, X. S. Li, Y. Zhang and Y. Wang, *Energ Fuel*, 2012, 26, 6300-6310.
223. G. Li, X. S. Li, B. Yang, L. P. Duan, N. S. Huang, Y. Zhang and L. G. Tang, *Appl Energ*, 2013, 112, 1303-1310.
224. G. Li, G. J. Moridis, K. Zhang and X. S. Li, *J Petrol Sci Eng*, 2011, 77, 49-68.
225. X. S. Li, Y. Wang, G. Li and Y. Zhang, *Energ Fuel*, 2012, 26, 1124-1134.
226. X. S. Li, B. Yang, L. P. Duan, G. Li, N. S. Huang and Y. Zhang, *Appl Energ*, 2013, 112, 1233-1240.
227. B. Liu, Q. Yuan, K. H. Su, X. Yang, B. C. Wu, C. Y. Sun and G. J. Chen, *Energies*, 2012, 5, 466-493.
228. L. G. Liu, J. F. Zhao, C. X. Cheng, Y. C. Song, W. G. Liu, Y. Liu, Y. Zhang and Z. Yang, *Proceedings of the Asme 31st International Conference on Ocean, Offshore and Arctic Engineering, 2012, Vol 6*, 2012, 697-702.
229. F. L. Ning, N. Y. Wu, G. S. Jiang, L. Zhang, J. A. Guan, Y. B. Yu and F. L. Tang, *Energies*, 2010, 3, 1861-1879.
230. H. Oyama, Y. Konno, Y. Masuda and H. Narita, *Energ Fuel*, 2009, 23, 4995-5002.
231. H. Oyama, Y. Konno, K. Suzuki and J. Nagao, *Chem Eng Sci*, 2012, 68, 595-605.
232. J. Phirani and K. K. Mohanty, *Chem Eng Sci*, 2009, 64, 2361-2369.
233. Y. Sakamoto, T. Komai, T. Kawamura, N. Tenma and T. Yamaguchi, *Proceedings of the Seventh (2007) Isope Ocean Mining (& Gas Hydrates) Symposium*, 2007, 102-107.
234. J. M. Schicks, E. Spangenberg, R. Giese, M. Luzi-Helbing, M. Priegnitz and B. Beeskow-Strauch, *Energies*, 2013, 6, 3002-3016.
235. Z. Su, Y. He, N. Y. Wu, K. N. Zhang and G. J. Moridis, *J Petrol Sci Eng*, 2012, 86-87, 87-98.
236. Z. Su, G. J. Moridis, K. N. Zhang and N. Y. Wu, *J Petrol Sci Eng*, 2012, 86-87, 54-61.
237. W. M. Sung, H. Lee, S. Kim and H. Kang, *Energ Source*, 2003, 25, 845-856.
238. W. M. Sung, H. Lee, H. Lee and C. Lee, *Energ Source*, 2002, 24, 499-512.
239. W. F. Waite, T. J. Kneafsey, W. J. Winters and D. H. Mason, *J Geophys Res-Sol Ea*, 2008, 113.
240. Q. B. Wu, Y. M. Wang and J. Zhan, *J Nat Gas Chem*, 2012, 21, 91-97.
241. L. J. Xiong, X. S. Li, Y. Wang and C. G. Xu, *Energies*, 2012, 5, 518-530.
242. K. Yamamoto and M. Kurihara, *Poro-Mechanics Iv*, 2009, 947-952.
243. S. W. Yang, X. M. Lang, Y. H. Wang, Y. G. Wen and S. S. Fan, *Energ Convers Manage*, 2014,

77, 298-305.

244. T. Yu, W. G. Liu, J. F. Zhao, Y. C. Song and Y. Liu, *Proceedings of the Asme 31st International Conference on Ocean, Offshore and Arctic Engineering, 2012, Vol 6*, 2012, 743-747.
245. Q. Yuan, C. Y. Sun, X. H. Wang, X. Y. Zeng, X. Yang, B. Liu, Z. W. Ma, Q. P. Li, L. Feng and G. J. Chen, *Fuel*, 2013, 106, 417-424.
246. Q. Yuan, C. Y. Sun, X. Yang, P. C. Ma, Z. W. Ma, B. Liu, Q. L. Ma, L. Y. Yang and G. J. Chen, *Energy*, 2012, 40, 47-58.
247. J. Zhao, D. Shi and Y. Zhao, *Oil Gas Sci Technol*, 2012, 67, 379-385.
248. J. F. Zhao, C. C. Ye, Y. C. Song, W. G. Liu, C. X. Cheng, Y. Liu, Y. Zhang, D. Y. Wang and X. K. Ruan, *Ind Eng Chem Res*, 2012, 51, 3108-3118.
249. J. F. Zhao, T. Yu, Y. C. Song, D. Liu, W. G. Liu, Y. Liu, M. J. Yang, X. K. Ruan and Y. H. Li, *Energy*, 2013, 52, 308-319.
250. Z. W. Zhao and X. C. Shang, *Int J Numer Anal Met*, 2010, 34, 1831-1845.
251. H. F. Liang, Y. C. Song and Y. J. Chen, *Energ Convers Manage*, 2010, 51, 1883-1890.
252. Y. Liu, M. Strumendo and H. Arastoopour, *Ind Eng Chem Res*, 2008, 47, 2817-2828.
253. Y. Liu, M. Strumendo and H. Arastoopour, *Ind Eng Chem Res*, 2009, 48, 2451-2464.
254. E. M. Myshakin, M. Gaddipati, K. Rose and B. J. Anderson, *Mar Petrol Geol*, 2012, 34, 169-185.
255. K. Nazridoust and G. Ahmadi, *Chem Eng Sci*, 2007, 62, 6155-6177.
256. O. Ors and C. Sinayuc, *J Petrol Sci Eng*, 2014, 119, 156-162.
257. D. Peters, M. S. Selim and E. D. Sloan, *Ann Ny Acad Sci*, 2000, 912, 304-313.
258. X. K. Ruan, Y. C. Song, H. F. Liang, M. J. Yang and B. L. Dou, *Energ Fuel*, 2012, 26, 1681-1694.
259. X. K. Ruan, Y. C. Song, J. F. Zhao, H. F. Liang, M. J. Yang and Y. H. Li, *Energies*, 2012, 5, 438-458.
260. X. K. Ruan, M. J. Yang, Y. C. Song, H. F. Liang and Y. H. Li, *J Nat Gas Chem*, 2012, 21, 381-392.
261. Y. Sakamoto, M. Kakumoto, K. Miyazaki, N. Tenma, T. Komai, T. Yamaguchi, M. Shimokawara and K. Ohga, *Int J Offshore Polar*, 2009, 19, 124-134.
262. W. Y. Sean, T. Sato, A. Yamasaki and F. Kiyono, *Aiche J*, 2007, 53, 2148-2160.
263. M. D. White, S. K. Wurstner and B. P. McGrail, *Mar Petrol Geol*, 2011, 28, 546-560.
264. J. W. Jung, *Am Mineral*, 2014, 99, 253-254.
265. K. F. Yan, X. S. Li, Z. Y. Chen, B. Li and C. G. Xu, *Mol Simulat*, 2013, 39, 251-260.
266. T. Toki, Y. Uehara, K. Kinjo, A. Ijiri, U. Tsunogai, H. Tomaru and J. Ashi, *Geochem J*, 2012, 46, 89-106.
267. Y. Seo, S. Lee and J. Lee, *Chem Engineer Trans*, 2013, 32, 163-168.
268. J. W. Pohlman, M. Kaneko, V. B. Heuer, R. B. Coffin and M. Whiticar, *Earth Planet Sc Lett*, 2009, 287, 504-512.
269. X. S. Li, B. Yang, G. Li and B. Li, *Ind Eng Chem Res*, 2012, 51, 4424-4432.
270. S. Lee, S. Park, Y. Lee and Y. Seo, *Chem Eng J*, 2013, 225, 636-640.
271. B. R. Lee, C. A. Koh and A. K. Sum, *Phys Chem Chem Phys*, 2014, 16, 14922-14927.
272. J. W. Jung, D. N. Espinoza and J. C. Santamarina, *J Geophys Res-Sol Ea*, 2010, 115.
273. D. N. Espinoza and J. C. Santamarina, *Int J Greenh Gas Con*, 2011, 5, 1031-1038.
274. C. Deusner, N. Bigalke, E. Kossel and M. Haeckel, *Energies*, 2012, 5, 2112-2140.

275. Y. Wang, X. S. Li, G. Li, N. S. Huang and J. C. Feng, *Fuel*, 2014, 117, 688-696.
276. N. Temma, Y. Sakamoto, T. Komai, T. Yamaguchi, G. Zyvoloski and R. Pawar, *Proceedings of the Sixteenth (2006) International Offshore and Polar Engineering Conference, Vol 1*, 2006, 299-303.
277. P. Taboada-Serrano, S. Ulrich, P. Szymcek, S. D. McCallum, T. J. Phelps, A. Palumbo and C. Tsouris, *Ind Eng Chem Res*, 2009, 48, 6448-6452.
278. K. Sasaki, S. Ono, Y. Sugai, T. Ebinuma, H. Narita and T. Yamaguchi, *J Can Petrol Technol*, 2009, 48, 21-26.
279. Y. Sakamoto, T. Komai, Y. Kawabe, N. Tenma and T. Yamaguchi, *Proceedings of the Fourteenth (2004) International Offshore and Polar Engineering Conference, Vol 1*, 2004, 52-55.
280. D. D. Link, N. English and C. Taylor, *Abstr Pap Am Chem S*, 2005, 229, U593-U593.
281. J. M. Gong, Z. M. Cao, J. W. Chen, M. Zhang, J. Li and G. F. Yang, *Sci China Ser D*, 2009, 52, 22-28.
282. S. Gerami and M. Pooladi-Darvish, *J Petrol Sci Eng*, 2007, 56, 146-164.
283. M. J. Castaldi, Y. Zhou and T. M. Yegulalp, *J Petrol Sci Eng*, 2007, 56, 176-185.
284. G. Ahmadi, C. Ji and D. H. Smith, *J Petrol Sci Eng*, 2007, 58, 245-258.
285. G. Ahmadi, C. Ji and D. H. Smith, *J Petrol Sci Eng*, 2004, 41, 269-285.
286. T. Uchida, S. Takeya, T. Ebinuma and H. Narita, *Greenhouse Gas Control Technologies*, 2001, 523-527.
287. J. H. Yoon, T. Kawamura, Y. Yamamoto and T. Komai, *J Phys Chem A*, 2004, 108, 5057-5059.
288. E. M. Yezdimer, P. T. Cummings and A. A. Chialvo, *J Phys Chem A*, 2002, 106, 7982-7987.
289. V. P. Voronov, E. E. Gorodetskii and A. R. Muratov, *J Phys Chem B*, 2010, 114, 12314-12318.
290. Y. X. Qi and H. Zhang, *Advanced Materials Science and Technology, Pts 1-2*, 2011, 181-182, 310-315.
291. R. Martos-Villa, M. P. Mata and C. I. Sainz-Diaz, *J Mol Graph Model*, 2014, 49, 80-90.
292. Z. Z. Li, X. Q. Guo, L. Y. Yang and X. N. Ma, *Petrol Sci*, 2009, 6, 426-432.
293. S. Lee, Y. Lee, J. Lee, H. Lee and Y. Seo, *Environ Sci Technol*, 2013, 47, 13184-13190.
294. H. Lee, Y. Seo, Y. T. Seo, D. Y. Kim, I. L. Moudrakovski and J. A. Ripmeester, *Stud Surf Sci Catal*, 2004, 153, 495-500.
295. D. S. Bai, X. R. Zhang, G. J. Chen and W. C. Wang, *Energ Environ Sci*, 2012, 5, 7033-7041.

FIGURE AND TABLE CAPTIONS

Permissions acknowledgment

We greatly thank the copyright holders of the following material (figures) for permission to reproduce extracts and artwork in this work.

Maranori Kurihara (Department of Resources and Environmental Engineering, Waseda University 3-4-1 Okubo, Shinjuku-ku, Tokyo 169-8555, Japan)
Extracts from: Gas production from methane hydrate reservoirs (by Masanori Kurihara, Hisanao Ouchi and Hideo Narita), from Proceedings of the 7th International Conferences on Gas Hydrates (ICGH 2011)

Ray Boswell (US DOE/NETL) and **Tim Collett** (USGS)
Extracts from: The gas hydrates resource pyramid (by Ray Boswell and Tim Collett), from Fire In the Ice, edited US DOE.

Yi Wang, Xiaosen Li, Gang Li, Jinchun Feng, Zhaoyang Chen, Yu Zhang (Key laboratory of Gay Hydrate, Chinese Academy of Sciences, Guangzhou 510640, PR China)
Extracts from: 3-D experimental investigation of heat transfer during gas production form hydrate pilot-scale hydrate simulator, from Proceedings of the 8th International Conference on Gas Hydrates (ICGH-2014).

S. Hancock (SPE, RPS Energy Canada), **G. Moridis** (SPE, Lawrence Berkley National Laboratory), **S. Wilson** (SPE, Ryder Scott Company), **A. Robertson** (SPE, RPS Energy Canada)
Extracts from: Well design requirements for deepwater and arctic onshore gas hydrate production wells, from OTC 21015, edited by Offshore Technology Conference

Timothy S. Collett (USGS)
Extracts from: International Gas Hydrate Research (March 2014) from
http://energy.gov/sites/prod/files/2014/04/f14/International_Review_USGS_Collett%5B1%5D.pdf

Figure caption

FIGURE 1. Type of NGH reservoir
Figure reproduced with permission from reference 60

FIGURE 2.NGH deposits in the world
Figure reproduced with permission from reference 54

FIGURE 3. The hydrate resource pyramid modified from Boswell and Collett (2006)
Figure adapted with permission from reference 59

FIGURE 4. Schematic over class 1~3 types of the NGH deposits

Figure reproduced with permission from reference 60

FIGURE 5. Principle of NGH dissociation
Figure adapted with permission from reference 60

FIGURE 6. Schematic of three main gas production methods
Figure adapted with permission from references 60 and 208

FIGURE 7. Schematic of phases and components in a kinetic model

FIGURE 8. Outline of International gas hydrate research in the world
Figure adapted with permission from Reference 204

FIGURE 9. Schematic of experimental apparatus with PHS
Figure reproduced with permission from reference 25

FIGURE 10. Schematic of layers and well design of PHS
Figure reproduced with permission from reference 25

Table caption

Table 1. List of the studies of methane production from natural gas hydrate by different methods

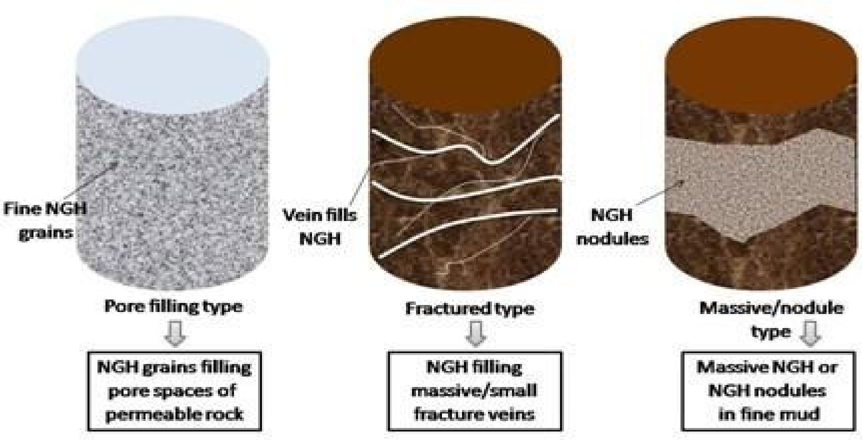

Figure 1. Type of NGH reservoir[60].

Figuire 2.NGH deposits in the world.

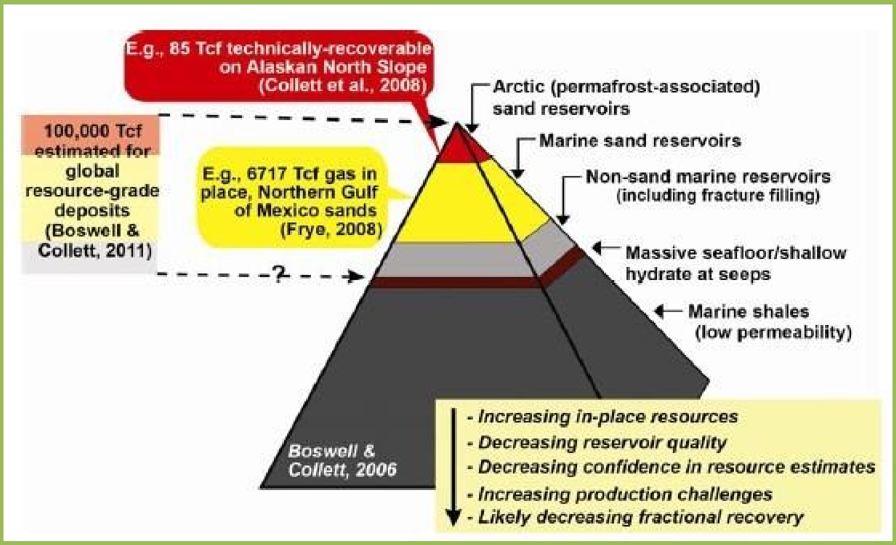

Figure 3. The hydrate resource pyramid modified from Boswell and Collett (2006)[58].

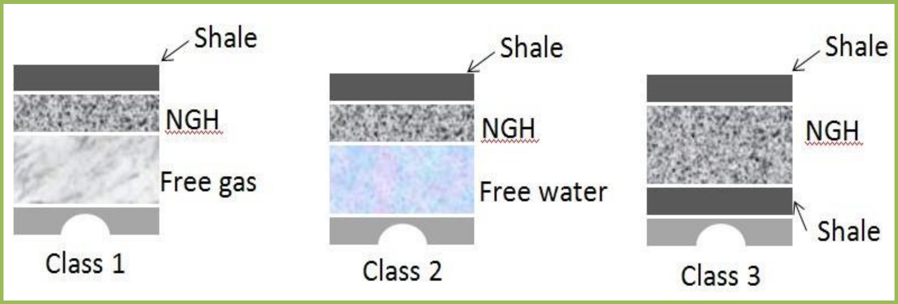

Figure 4. Schematic over class 1~3 types of the NGH deposits[60].

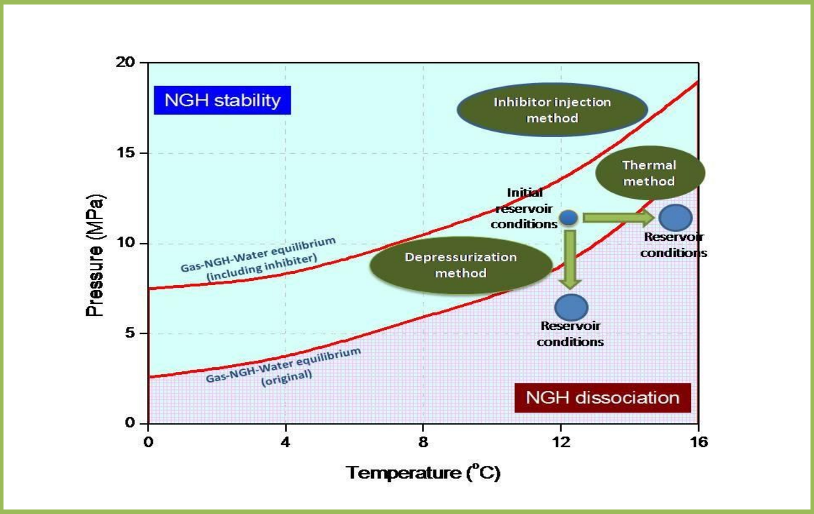

Figure 5. Principle of NGH dissociation[60].

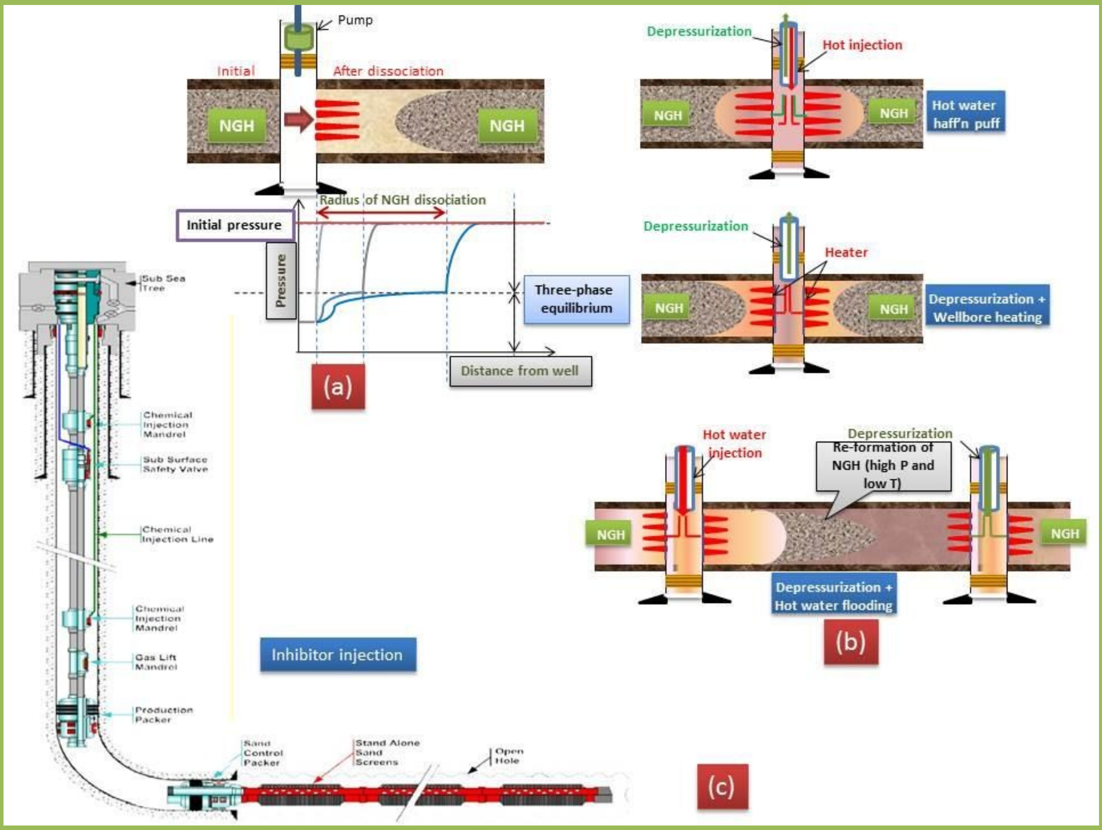

Figure 6. Schematic of three main gas production methods[60, 208].

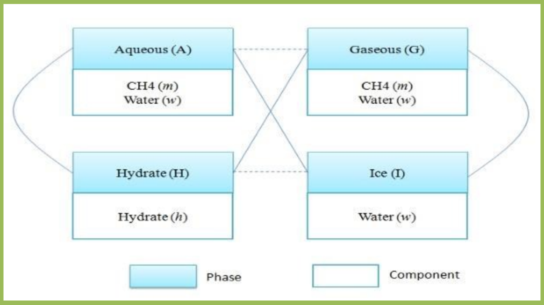

Figure 7. Schematic of phases and components in a kinetic model.

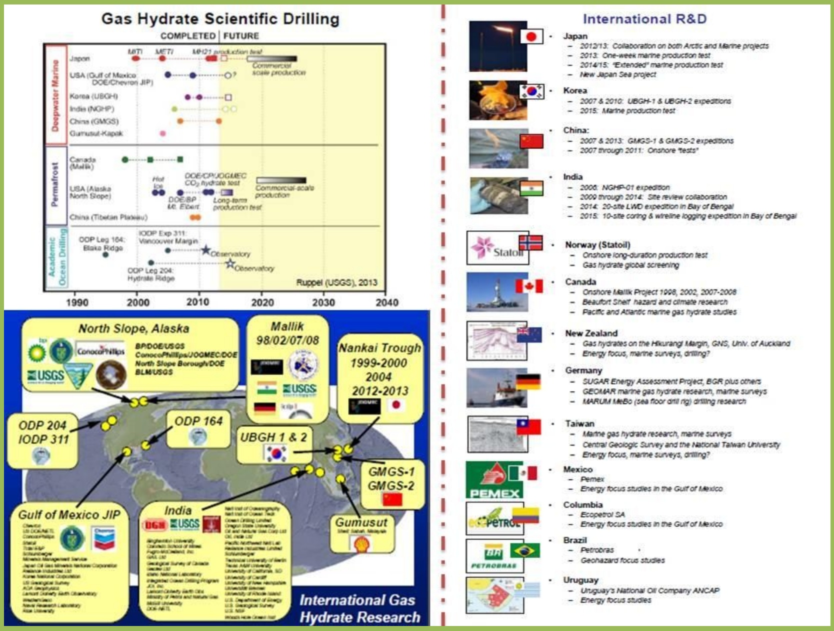

Figure 8. Outline of International gas hydrate research in the world[204].

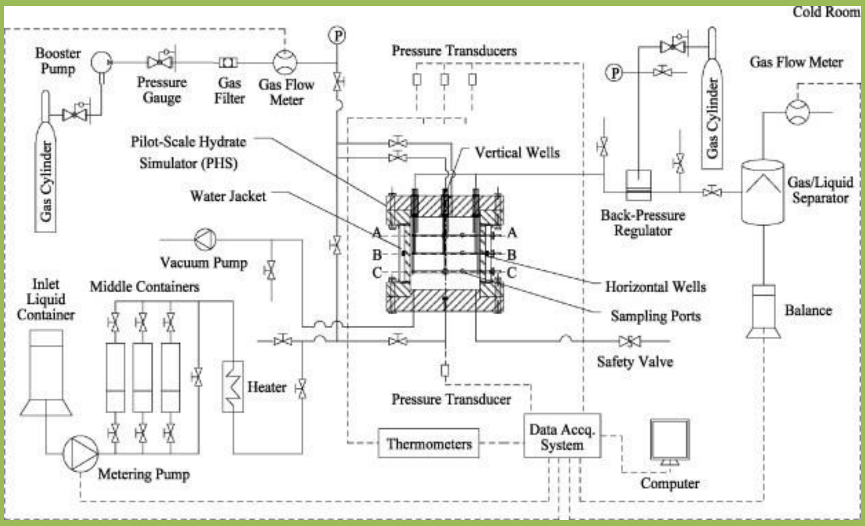

Figure 9. Schematic of experimental apparatus with PHS [25].

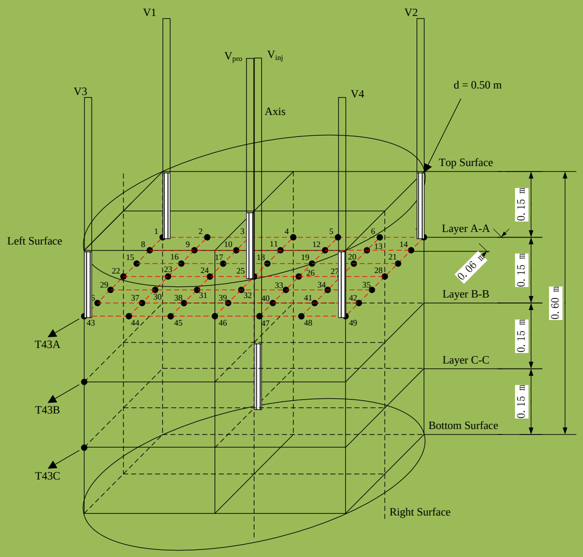

Figure 10. Schematic of layers and well design of PHS [25].

Table 1. List of the studies of methane production from NGH by different methods

Item	method	literature	Subject
1	Depressurization	Li et al.[209]	Depressurization induced gas production from hydrate deposits with low gas saturation in a pilot-scale hydrate simulator
2	Depressurization	Shahbazi et al.[210]	Behavior of Depressurization in Type III Hydrate Reservoirs
3	Depressurization	Chejara et al.[211]	Simulations of long term methane hydrate dissociation by pressure reduction using an extended RetrasoCodeBright simulator
4	Depressurization combined with heating	Falser et al.[212]	Increased Gas Production from Hydrates by Combining Depressurization with Heating of the Wellbore
5	Depressurization combined with heating	Feng et al.[213]	Evolution of Hydrate Dissociation by Warm Brine Stimulation Combined Depressurization in the South China Sea
6	Thermal stimulation	Fitzgerald & Castaldi[214]	Thermal Stimulation Based Methane Production from Hydrate Bearing Quartz Sediment
7	Depressurization	Haligva et al.[13]	Recovery of Methane from a Variable-Volume Bed of Silica Sand/Hydrate by Depressurization
8	Depressurization	Ji et al.[215]	Natural gas production from hydrate decomposition by depressurization
9	Depressurization	Jiang et al.[216]	Sensitivity analysis of gas production from Class I hydrate reservoir by depressurization
10	Thermal stimulation	Kawamura et al.[217]	Experimental study on steam injection method using methane hydrate core samples
11	Inhibitor or Steam injection combined with depressurization	Kawamura et al.[218]	Dissociation Behavior of Hydrate Core Sample Using Thermodynamic Inhibitor-Part 3. Inhibitor or Steam Injection Combined with Depressurization and High-Concentration Inhibitor Injection
12	Inhibitor injection	Kawamura et al.[219]	Dissociation experiment of hydrate core sample using thermodynamic inhibitors - Part 2
13	Depressurization	Kim et al.[220]	Depressurization experiment of pressure cores from the central Ulleung Basin, East Sea: Insights into gas chemistry
14	Depressurization	Konno et al.[221]	Key Factors for Depressurization-Induced Gas Production from Oceanic Methane Hydrates
15	Depressurization	Lee et al.[74]	An experimental study on the productivity of dissociated gas from gas hydrate by depressurization scheme
16	Inhibitor combined with Depressurization	Li et al.[24]	Gas Production from Methane Hydrate in a Pilot-Scale Hydrate Simulator Using the Huff and

			Puff Method by Experimental and Numerical Studies
17	Depressurization	Li et al.[222]	Experimental and Numerical Studies on Gas Production from Methane Hydrate in Porous Media by Depressurization in Pilot-Scale Hydrate Simulator
18	Steam injection combined with depressurization	Li et al.[96]	Production behavior of methane hydrate in porous media using huff and puff method in a novel three-dimensional simulator
19	Steam injection combined with depressurization	Li et al.[223]	The use of dual horizontal wells in gas production from hydrate accumulations
20	Steam injection combined with depressurization	Li et al.[224]	The use of huff and puff method in a single horizontal well in gas production from marine gas hydrate deposits in the Shenhu Area of South China Sea
21	Steam injection	Li et al.[225]	Experimental Investigations into Gas Production Behaviors from Methane Hydrate with Different Methods in a Cubic Hydrate Simulator
22	Depressurization combined with heat injection	Li et al.[226]	Experimental study on gas production from methane hydrate in porous media by SAGD method
23	Depressurization combined with heat injection	Li et al.[97]	Experimental study on gas production from methane hydrate in porous media by huff and puff method in Pilot-Scale Hydrate Simulator
24	Depressurization	Li et al.	Experimental investigation into gas production from methane hydrate in sediment by depressurization in a novel pilot-scale hydrate simulator
25	Depressurization	Li et al.[84]	Experimental Investigation into the Production Behavior of Methane Hydrate in Porous Sediment by Depressurization with a Novel Three-Dimensional Cubic Hydrate Simulator
26	Depressurization, inhibitor, heat injection	Liu et al.[227]	Experimental Simulation of the Exploitation of Natural Gas Hydrate
27	Depressurization and combined method	Liu et al.[228]	Experimental Study of Gas Production from Methane Hydrate by Depressurization and Combination Method under Different Hydrate Saturations
28	Depressurization	Moridis et al.[19]	Gas production potential of disperse low-saturation hydrate accumulations in oceanic sediments
29	Solar energy heating and depressurization	Ning et al.[229]	A Method to Use Solar Energy for the Production of Gas from Marine Hydrate-Bearing Sediments: A Case Study on the Shenhu Area

30	Depressurization	Oyama et al.[230]	Dependence of Depressurization-Induced Dissociation of Methane Hydrate Bearing Laboratory Cores on Heat Transfer
31	Depressurization	Oyama et al.[231]	Depressurized dissociation of methane-hydrate-bearing natural cores with low permeability
32	Hot water injection	Phirani et al.[232]	Warm water flooding of confined gas hydrate reservoirs
33	Depressurization	Sakamoto et al.[233]	Field scale simulation for the effect of relative permeability on dissociation and gas production behavior during depressurization process of methane hydrate in marine sediments
34	Thermal stimulation	Schicks et al.[234]	A Counter-Current Heat-Exchange Reactor for the Thermal Stimulation of Hydrate-Bearing Sediments
35	Depressurization	Su et al.[235]	Evaluation on gas production potential from laminar hydrate deposits in Shenhu Area of South China Sea through depressurization using vertical wells
36	Steam injection	Su et al.[236]	A huff-and-puff production of gas hydrate deposits in Shenhu area of South China Sea through a vertical well
37	Depressurization	Sun et al.[79]	1-D modeling of hydrate depressurization in porous media
38	Depressurization	Sung et al.[237]	Experimental investigation of production behaviors of methane hydrate saturated in porous rock
39	Inhibitor injection	Sung et al.[238]	Numerical study for production performances of a methane hydrate reservoir stimulated by inhibitor injection
40	Depressurization	Tang et al.[72]	Control mechanisms for gas hydrate production by depressurization in different scale hydrate reservoirs
41	Depressurization	Waite et al.[239]	Physical property changes in hydrate-bearing sediment due to depressurization and subsequent repressurization
42	Depressurization and heating	Wu et al.[240]	Effect of rapidly depressurizing and rising temperature on methane hydrate dissociation
43	Depressurization	Xiong et al.[241]	Experimental Study on Methane Hydrate Dissociation by Depressurization in Porous Sediments
44	Depressurization	Yamamoto et al.[242]	Gas Hydrate Production from Geological Formations as Transport Phenomena
45	Molecular dynamics simulation/depressurization	Yan et al.	Molecular dynamics simulation of methane hydrate dissociation by depressurisation
46	Numerical	Yang et al.[243]	Numerical simulation of Class 3 hydrate reservoirs

	simulation/depressurization		exploiting using horizontal well by depressurization and thermal co-stimulation
47	Depressurization	Yang et al.[83]	A three-dimensional study on the formation and dissociation of methane hydrate in porous sediment by depressurization
48	Hot-water cyclic injection	Yang et al.[92]	Experimental Study on Gas Production from Methane Hydrate-Bearing Sand by Hot-Water Cyclic Injection
49	Numerical simulation/depressurization	Yu et al.[244]	Numerical Simulation on Natural Gas Production from Gas Hydrate Dissociation by Depressurization
50	CO_2 replacement	Yuan et al.[62]	Methane recovery from natural gas hydrate in porous sediment using pressurized liquid CO_2
51	Heat and inhibitor injection	Yuan et al.[245]	Experimental study of gas production from hydrate dissociation with continuous injection mode using a three-dimensional quiescent reactor
52	CO_2 replacement	Yuan et al.[246]	Recovery of methane from hydrate reservoir with gaseous carbon dioxide using a three-dimensional middle-size reactor
53	Mathematical model and simulation/depressurization	Zhao et al.[247]	Mathematical Model and Simulation of Gas Hydrate Reservoir Decomposition by Depressurization
54	Numerical simulation/depressurization	Zhao et al.[248]	Numerical Simulation and Analysis of Water Phase Effect on Methane Hydrate Dissociation by Depressurization
55	Numerical simulation/depressurization	Zhao et al.[249]	Numerical simulation of gas production from hydrate deposits using a single vertical well by depressurization in the Qilian Mountain permafrost, Qinghai-Tibet Plateau, China
56	Depressurization	Zhao et al.[250]	Analysis for temperature and pressure fields in process of hydrate dissociation by depressurization
57	Numerical simulation/depressurization, inhibitor or heat injection	Kurihara et al.[98]	Prediction of Gas Productivity From Eastern Nankai Trough Methane-Hydrate Reservoirs
58	Numerical simulation/depressurization	Liang et al.[251]	Numerical simulation for laboratory-scale methane hydrate dissociation by depressurization
59	Numerical simulation/depressurization, inhibitor or heat injection	Liu et al.[252]	Numerical simulation of methane production from a methane hydrate formation
60	Depressurization and thermal injection	Liu et al.[253]	Simulation of Methane Production from Hydrates by Depressurization and Thermal Stimulation
61	Numerical simulation/depressurization	Mori dis[17]	Numerical studies of gas production from Class 2 and Class 3 hydrate accumulations at the Mallik site, Mackenzie Delta, Canada
62	Numerical	Moridis et al.[8]	Numerical studies of gas production from several

	simulation/depressurization and thermal stimulation		CH_4 hydrate zones at the Mallik site, Mackenzie Delta, Canada
63	Numerical simulation/depressurization	Myshakin et al.[254]	Numerical simulations of depressurization-induced gas production from gas hydrate reservoirs at the Walker Ridge 313 site, northern Gulf of Mexico
64	Computational modeling/depressurization	Nazridoust & Ahmadi[255]	Computational modeling of methane hydrate dissociation in a sandstone core
65	CO_2 replacement	Ors & Sinayuc[256]	An experimental study on the CO_2-CH_4 swap process between gaseous CO_2 and CH_4 hydrate in porous media
66	Depressurization	Peters et al.[257]	Hydrate dissociation in pipelines by two-sided depressurization - Experiment and model
67	Numerical simulation/depressurization	Ruan et al.[258]	Numerical Simulation of the Gas Production Behavior of Hydrate Dissociation by Depressurization in Hydrate-Bearing Porous Medium
68	Numerical simulation/depressurization	Ruan et al.[259]	Numerical Simulation of Methane Production from Hydrates Induced by Different Depressurizing Approaches
69	Numerical simulation/depressurization	Ruan et al.[260]	Numerical studies of hydrate dissociation and gas production behavior in porous media during depressurization process
70	Numerical simulation/depressurization	Sakamoto et al.[261]	Numerical Study on Dissociation of Methane Hydrate and Gas Production Behavior in Laboratory-Scale Experiments for Depressurization: Part 3-Numerical Study on Estimation of Permeability in Methane Hydrate Reservoir
71	Computational modeling/depressurization	Sean et al.[262]	CFD and experimental study on methane hydrate dissociation. Part II. General cases
72	Numerical simulation/CO_2 injection	White et al.[263]	Numerical studies of methane production from Class 1 gas hydrate accumulations enhanced with carbon dioxide injection
73	CO_2 replacement	Jung[264]	Entrapping CO_2, while recovering methane
74	Molecular dynamics simulation/depressurization	Yan et al.[265]	Molecular dynamics simulation of methane hydrate dissociation by depressurization
75	Depressurization	Toki et al.[266]	Methane production and accumulation in the Nankai accretionary prism: Results from IODP Expeditions 315 and 316
76	CO_2 replacement	Seo et al.[267]	Experimental Verification of Methane Replacement in Gas Hydrates by Carbon Dioxide
77	CO_2 replacement	Pohlman et al.[268]	Methane sources and production in the northern Cascadia margin gas hydrate system
78	Numerical simulation/depressurization	Li et al.[269]	Numerical Simulation of Gas Production from Natural Gas Hydrate Using a Single Horizontal Well

			by Depressurization in Qilian Mountain Permafrost
79	CO_2 replacement	Lee et al.[270]	Thermodynamic and C-13 NMR spectroscopic verification of methane-carbon dioxide replacement in natural gas hydrates
80	CO_2 replacement	Lee et al.[271]	Quantitative measurement and mechanisms for CH_4 production from hydrates with the injection of liquid CO_2
81	CO_2 replacement	Jung et al.[272]	Properties and phenomena relevant to CH_4-CO_2 replacement in hydrate-bearing sediments
82	CO_2 replacement	Espinoza & Santamarina[273]	P-wave monitoring of hydrate-bearing sand during CH_4-CO_2 replacement
83	CO_2 replacement	Deusner et al.[274]	Methane Production from Gas Hydrate Deposits through Injection of Supercritical CO_2
84	Depressurization combined with heat injection	Wang et al.[94]	Experimental investigation into scaling models of methane hydrate reservoir
85	Thermal huff'n puff	Wang et al.[275]	Experimental study on the hydrate dissociation in porous media by five-spot thermal huff and puff method
86	Numerical simulation/depressurization	Temma et al.[276]	Numerical simulation of gas hydrate dissociation in artificial sediment
87	CO_2 replacement	Taboada-Serrano et al.[277]	Multiphase, Microdispersion Reactor for the Continuous Production of Methane Gas Hydrate
88	Depressurization	Su et al.[82]	Experimental investigation of methane hydrate decomposition by depressurizing in porous media with 3-Dimension device
89	Hot water injection	Sasaki et al.[278]	Gas Production System From Methane Hydrate Layers by Hot Water Injection Using Dual Horizontal Wells
90	Heat stimulation	Sakamoto et al.[279]	Gas hydrate extraction from marine sediments by heat stimulation method
91	Thermal stimulation	Pang et al.[89]	Methane hydrate dissociation experiment in a middle-sized quiescent reactor using thermal method
92	Depressurization	Link et al.[280]	Methane hydrate research at NETL, research to make methane production from hydrates a reality
93	CO_2/CO_2-N_2 replacement	Koh et al.[180]	Recovery of Methane from Gas Hydrates Intercalated within Natural Sediments Using CO_2 and a CO_2/N_2 Gas Mixture
94	Thermal stimulation	Gong et al.[281]	Simulation experiments on gas production from hydrate-bearing sediments
95	Depressurization	Gerami & Pooladi-Darvish[282]	Predicting gas generation by depressurization of gas hydrates where the sharp-interface assumption is not valid
96	Mathematical modeling	Gamwo & Liu[196]	Mathematical Modeling and Numerical Simulation

	and numerical simulation		of Methane Production in a Hydrate Reservoir
97	Thermal stimulation	Castaldi[283]	Down-hole combustion method for gas production from methane hydrates
98	Depressurization	Ahmadi et al.[21]	Production of natural gas from methane hydrate by a constant downhole pressure well
99	Computation modeling	Ahmadi et al.[284]	Natural gas production from hydrate dissociation: An axisymmetric model
100	Numerical simulation	Ahmadi et al.[285]	Numerical solution for natural gas production from methane hydrate dissociation
101	CO_2 replacement	Uchida et al.[286]	Replacing methane with CO_2 in clathrate hydrate: Observations using Raman spectroscopy
102	CO_2 replacement	Zhou et al.[49]	Replacement of methane from quartz sand-bearing hydrate with carbon dioxide-in-water emulsion
103	CO_2 replacement	Zhou et al.[35]	Determination of appropriate condition on replacing methane from hydrate with carbon dioxide
104	CO2 replacement	Yoon et al.[287]	Transformation of methane hydrate to carbon dioxide hydrate: In situ Raman spectroscopic observations
105	CO2 replacement	Yezdimer et al.[288]	Determination of the Gibbs free energy of gas replacement in SI clathrate hydrates by molecular simulation
106	CO_2 replacement	Voronov et al.[289]	Experimental Study of Methane Replacement in Gas Hydrate by Carbon Dioxide
107	Molecular dynamics simulation/replacement	Tung et al.[40]	In Situ Methane Recovery and Carbon Dioxide Sequestration in Methane Hydrates: A Molecular Dynamics Simulation Study
108	CO_2 replacement	Qi & Zhang[290]	MD Simulation of CO_2-CH_4 Mixed Hydrate on Crystal Structure and Stability
109	Molecular dynamics simulation/replacement	Qi et al.[181]	Molecular dynamics simulation of replacement of CH_4 in hydrate with CO_2
110	CO_2 replacement	Ota et al.[136]	Macro and microscopic CH_4-CO_2 replacement in CH4 hydrate under pressurized CO_2
111	CO_2 replacement	Ota et al.[44]	Replacement of CH_4 in the hydrate by use of liquid CO_2
112	CO_2 replacement	Ota et al.[38]	Methane recovery from methane hydrate using pressurized CO_2
113	CO_2 replacement	Martos-Villa et al.[291]	Characterization of CO_2 and mixed methane/CO_2 hydrates intercalated in smectites by means of atomistic calculations
114	CO_2 replacement	Li et al.[292]	Exploitation of methane in the hydrate by use of carbon dioxide in the presence of sodium chloride
115	CO_2 replacement	Lee et al.[293]	Experimental Verification of Methane-Carbon Dioxide Replacement in Natural Gas Hydrates

			Using a Differential Scanning Calorimeter
116	CO_2 replacement	Lee et al.[294]	Replacement of methane hydrate by carbon dioxide: C-13 NMR study for studying a limit to the degree of substitution
117	Molecular dynamics simulation/replacement	Iwai et al.[42]	Molecular dynamics simulation of replacement of methane hydrate with carbon dioxide
118	Molecular dynamics simulation/replacement	Geng et al.[41]	Molecular Simulation of the Potential of Methane Reoccupation during the Replacement of Methane Hydrate by CO_2
119	CO_2 replacement	Bai et al.[295]	Replacement mechanism of methane hydrate with carbon dioxide from microsecond molecular dynamics simulations